

THIS REPORT HAS BEEN DELIMITED  
AND CLEARED FOR PUBLIC RELEASE  
UNDER DOD DIRECTIVE 5200.20 AND  
NO RESTRICTIONS ARE IMPOSED UPON  
ITS USE AND DISCLOSURE.

**DISTRIBUTION STATEMENT A**

APPROVED FOR PUBLIC RELEASE,  
DISTRIBUTION UNLIMITED.

Reproduced by

**Armed Services Technical Information Agency**  
**DOCUMENT SERVICE CENTER**

**KNOTT BUILDING, DAYTON, 2, OHIO**

**AD -**

**18442**

**UNCLASSIFIED**



# *Cosmic Ray Project*

## **APPLIED PHYSICS LABORATORY**

A DIVISION OF THE DEPARTMENT OF PHYSICS  
UNIVERSITY OF WASHINGTON

### **The Momentum Spectrum of Cosmic Rays at 3.4 Kilometers**

**TECHNICAL REPORT**

OFFICE OF NAVAL RESEARCH  
CONTRACT N8ONR52008

**Best  
Available  
Copy**

APPLIED PHYSICS LABORATORY  
UNIVERSITY OF WASHINGTON  
A Division of the Department of Physics

THE MOMENTUM SPECTRUM OF COSMIC  
RAYs AT 3.4 KILOMETERS

By J. E. Henderson, C. E. Miller, D. S. Potter\*  
J. Todd and A. W. Wotring\*\*

TECHNICAL REPORT  
OFFICE OF NAVY RESEARCH  
CONTRACT N8onr 52008

Acknowledgment is made to the Bureau of Ordnance,  
Navy Department for support of the early stages of  
this research under Contract NOrd 7818.

Approved

  
J. E. Henderson, Director  
Applied Physics Laboratory

\*The physical material of this report was presented by D. S. Potter as a dissertation in partial fulfillment of the requirements for the Degree of Doctor of Philosophy of the Graduate School of the University of Washington.

\*\*A portion of the instrumentation described in this report was used by A. W. Wotring as the basis for a thesis for the degree of Master of Science at the University of Washington.

### ACKNOWLEDGEMENT

The high altitude work described here was carried out on the grounds of the Climax Molybdenum Company at Remont Pass in Colorado. The generous cooperation of C. S. Abrams, General Manager, and other personnel of this company is gratefully acknowledged. Important contributions to the research have also been made by Don Eng, electronic technician, and Elmer Wright, instrument maker, for our staff.

	Page
DISCUSSION	67
Momentum Distribution	67
Positive Excess	76
Protons	80
SUMMARY	83
BIBLIOGRAPHY	84

## LIST OF PLATES

Plate		Page
I	THE CLOUD CHAMBER BEFORE ASSEMBLY	8
II	A MESON TRACK	12
III	A PROTON TRACK	13
IV	A SHOWER	14
V	THE MAGNET FACE SHOWING THE CLOUD CHAMBER, THE FLASH TUBES, AND THE GEIGER TUBES	15
VI	THE MAGNET CORE	17
VII	THE TEMPERATURE CONTROL CIRCUIT	20
VIII	THE MOTOR GENERATOR CONTROL CIRCUIT	22
IX	THE EVENT SELECTOR CIRCUIT	24
X	THE CLOUD CHAMBER CONTROL CIRCUIT	26
XI	THE PROGRAM UNIT CIRCUIT	30
XII	THE BINARY SCALE CIRCUIT	32
XIII	THE EXPEDITION BEFORE LEAVING SEATTLE	34
XIV	THE LOCATION ON FREMONT PASS, COLORADO	36
XV	THE EQUIPMENT IN THE RADAR TRUCK	37
XVI	THE EXPERIMENTAL ARRANGEMENT	38
XVII	THE COMPARATOR	43

Plate		Page
XVIII	THE EVANS LINKAGE SYSTEM	45
XIX	THE MOMENTUM SPECTRUM AT 3.4 KILOMETERS UNDER NO ABSORBER AND UNDER 5 CM OF LEAD ABSORPER	59
XX	THE MOMENTUM SPECTRUM AT 3.4 KILOMETERS UNDER 5 CM OF LEAD ABSORBER	60
XXI	THE MOMENTUM SPECTRUM OF HEAVILY IONIZING PARTICLES	63
XXII	THE MOMENTUM SPECTRUM AT SEA LEVEL	68
XXIII	THE MOMENTUM SPECTRUM AT 30,000 FEET	69
XXIV	THE TRANSFORMED INTEGRAL RANGE SPECTRUM AT 4350 METERS	73

## LIST OF TABLES

Table		Page
I	COINCIDENCE COUNTING RATES	39
II	TABULATION DATA OF THE NEGATIVE AND POSITIVE PARTICLES FOR THE NO-ABSORBER CASE AND FOR THE 5 CM LEAD CASE	64
III	THE DISTRIBUTION IN MOMENTUM FOR PARTICLES OF BOTH SIGNS FOR THE NO ABSORBER CASE AND FOR THE 5 CM LEAD ABSORBER CASE	65
IV	THE DISTRIBUTION IN MOMENTUM FOR POSITIVE AND NEGATIVE PARTICLES FOR THE 5 CM LEAD ABSORBER CASE	65
V	HEAVILY IONIZING TRACKS UNDER NO ABSORBER AND 5 CM LEAD ABSORBER	66



## THE MOMENTUM SPECTRUM OF COSMIC RAYS AT 3.4 KILOMETERS

### I. INTRODUCTION

Early in the history of the study of cosmic rays it became obvious that the radiation could be separated into two components differing in the degree of their penetration. This phenomenological distinction came about from the following experimental considerations. It was known that in the measurement of the intensity of cosmic radiation the introduction of a few centimeters of lead absorber would decrease the intensity markedly. After about ten centimeters of lead had been placed on top of the apparatus to filter the radiation it was found that the rate of decrease of cosmic ray intensity with further absorbing materials quite abruptly decreased in magnitude. The remaining radiation was little affected by the interposition of further absorbing materials. It thus appeared that there were two distinct components, a soft or nonpenetrating component which could be removed by about ten centimeters of

lead and the hard or penetrating component which was little affected by fairly large quantities of lead absorber.

A great deal of work was done on the soft component in the early stages of cosmic ray investigation. It was discovered that the soft component consisted essentially of electrons and low energy gamma rays in a cascade process. Both experimental and theoretical investigations were undertaken during the 1920s and were fairly successful in explaining the gross effects. Although even today a quantitative theoretical treatment of the soft component which completely explains the cascade process is lacking, the high order of success attained in a semi-quantitative way by the theoretical treatment indicates that at least the basic portion of the problem has been solved. It is to be expected that further refinement in experimental technique will require a more precise theory.

Work on the hard component has proceeded at a much slower rate until the last few years. At first the hard component was considered to consist of very high energy gamma rays. Their ability to penetrate large amounts of absorber might thus be explained. Some investigators found evidence for supporting the view that the gamma rays making up the hard component had essentially discrete energy levels and that the absorption coefficients for the hard component yielded to a natural interpretation based on the method of formation of the high energy gamma ray.

The discovery of the meson added a new interest to the field of cosmic rays. The work of Neddermeyer and Anderson (1) showed quite conclusively that mesons were extremely penetrating and had sufficient energy to produce the effects attributed to the hard component. The fact that mesons underwent a decay process with quite short half-life further complicated the problem.

A more detailed study of the hard component yielded the fact that no existing meson theory could account for the experimental evidence. Investigation of penetrating showers and their rate of decrease through the atmosphere gave an even larger discrepancy with theory.

Postwar research has led to the notion of a nuclear cascade process. This is a process in which nucleons traversing the atmosphere undergo collisions in a cascade type of reaction. The collision of one nucleon with a nucleus produces several more nucleons and other penetrating particles, such as mesons, which go on to form a hard or penetrating cascade. In order to understand this nuclear cascade process a great deal of information regarding the meson intensity and the nucleon intensity as functions of momentum had to be obtained. The number of nucleons at sea-level was known to be quite small, so that, although several investigators had experimentally determined the momentum spectrum at sea-level, little use could be made of this information with regard to nuclear

cascade processes. Some latitude work had been done, primarily by Anderson (2) and by Hall (3). Hall's work, however, involved the determination of an integral range spectrum. From this, by assuming that all of the radiation with which he dealt was mesonic, he computed a momentum spectrum for his altitude of observation, namely, 14,000 feet. As will be considered in the discussion, the work of Hall raised more questions than it answered. It was thought that, because of the necessity of making assumptions concerning the nature of the radiation in determining a momentum spectrum, the determination of this spectrum by Hall might be in error. The difficulty with Hall's work became even more pronounced when it was realized that, for such a spectrum to exist, a large amount of low energy mesons would have to be produced in a region between 14,000 and 15,000 feet.

All work concerning the rate of meson production done at that altitude and higher yielded production rates far smaller than that required by Hall. Since the rate of production of mesons undoubtedly is directly connected with the nucleon flux, the fact that Hall's spectrum required meson production almost necessitated a large nucleon flux, in direct contradiction to the assumptions he had made. It was essential, therefore, that a direct determination of the momentum spectrum be made, one that involved no assumptions concerning the particles involved. This is the basic objective of the

present experiment. Obviously, a cloud chamber in a magnetic field is the choice of instrumentation.

The only direct experimental measurement of the momentum spectrum with altitude which had been done in sufficient detail to warrant consideration was that of the California Institute of Technology group in 1947 at 30,000 feet (2). Due to the great difficulty in flying a magnetic cloud chamber, the entire field of data consisted of only 250 measured tracks. In order to settle the question of meson production and the momentum spectrum at high altitude it is necessary to carry out a rather lengthy program utilizing a magnetic cloud chamber at as high an altitude as possible. Since it was vital to obtain as large a field of data as possible, aircraft observation was not considered practical. With this limitation then, it appeared that the best which could be done was to make extensive measurements at about 12,000 feet.

The experiment which is the basis for this dissertation, and which was performed in 1948, had as its objective the determination of the momentum spectrum and some qualitative observations on the nucleonic component. It was felt that this experiment was perhaps the most significant experiment which could be performed with the existing equipment in order to advance our understanding of the hard component of cosmic rays.

## II. EXPERIMENTAL APPARATUS

The experimental apparatus used in obtaining the basic data for this investigation can be conveniently divided into two parts, (1) the cloud chamber and auxiliary equipment necessary to make it function, and (2) the equipment necessary to produce and maintain the magnetic field. The equipment associated with the cloud chamber must include some means of event selection and a control unit for conducting the sequence of operations necessary to operate a cloud chamber. The magnet which produces the field in which the chamber is located requires, in addition to a d-c generator, a cooling and temperature-control system to protect the chamber from temperature gradients and fluctuations. A somewhat more detailed account of the units used to perform these various functions will be included in the next few pages.

### A. Cloud Chamber

The cloud chamber used in this investigation is two and a half inches deep and seven inches in diameter with a useful illuminated depth of about one inch. In order to keep the necessary air gap in the magnet assembly to a minimum, the expansion mechanism is not mounted on the back of the chamber as is usually the case, but instead is placed outside the magnet structure and connected to the chamber by a ten-inch

brass tube two inches in diameter. Plate I shows the cloud chamber, including the connecting tube, with all the parts in their relative assembled positions just prior to assembly. The parts shown, from left to right, are as follows: the ten-inch brass connecting tube and back wall; the brass baffle plate; the velvet, which is normally stitched to the brass baffle plate; the glass cylinder, which forms the wall of the chamber; the brass ring which seats the "O" ring gaskets and also acts as the positive return for the clearing field; the glass cover plate; black masking paper to define the diameter of the chamber; and the end retaining ring. The chamber is held together by studs which are screwed into the stud holes along the outer portion of the back wall and extend through the end retaining ring. The nuts on the end of the studs then pull the retaining ring down and compress the "O" ring seals. After the chamber has been assembled with the backing plate and expansion mechanism (not shown), the chamber is evacuated, and the nuts on the ends of the studs may be further tightened without danger of cracking the glass.

The expansion mechanism utilizes a neoprene diaphragm which acts as a movable separator between the chamber gas and the backing air. The chamber is expanded by exhausting the backing air pressure to the atmosphere through a "pop valve," the amount of expansion being determined by the position of an adjustable backing plate which defines the total motion of the diaphragm and, hence, the total increase in the volume of

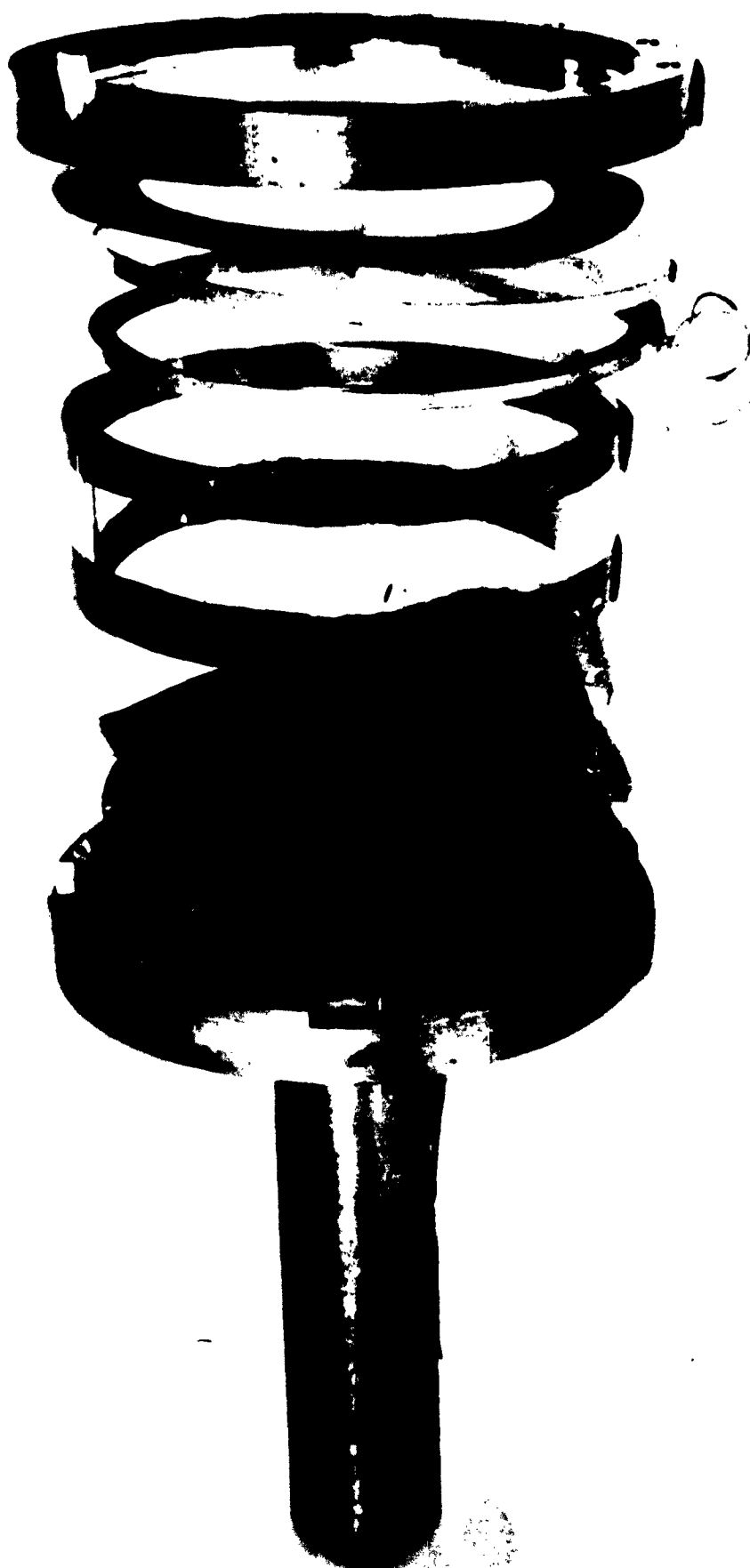


PLATE I. THE CLOUD CHAMBER BEFORE ASSEMBLY



the chamber. The "pop valve" is essentially a plunger which has a plate about an inch in diameter on its end. This plate closes a hole in the brass plate which confines the backing air pressure. The "pop valve" plate is held in position against the force of the backing air by a solenoid which acts on the plunger. When the holding current is released the plunger is accelerated by the pressure differential across the plate, and the valve opens. Since it is essential to have the valve operate quickly, the total mass of the moving elements has been kept as low as possible.

The chamber is filled with a mixture of argon gas and the saturated vapor of a 60-40 n-propyl alcohol-water mixture to a total pressure of 1.8 atmospheres. A backing air pressure six pounds greater than the filling pressure is used. The electronically operated "pop valve" is found to open within about two milliseconds after triggering, and from the track width (0.5 millimeters) and the minimum delay time after expansion before tracks can be photographed (0.02 seconds), the expansion time can be computed. The estimate made on the basis of the above data is a total time for expansion of 0.01 seconds. It has been found that, if the chamber is photographed about 0.05 seconds after expansion, the droplet size is sufficient for easy measurement of track curvature, but that not sufficient time has elapsed for turbulence in the gas flow to produce spurious curvature.

The introduction of the two-inch connecting tube between the chamber and the expansion mechanism in this chamber produces a structure resembling a Helmholtz oscillator. The sudden release of the backing air pressure, and the resulting movement of the neoprene diaphragm which increases the volume of the expansion side of the chamber, shock excites the resonator, and the pressure of the gas in the chamber proper then varies with time in accordance with a damped oscillation. As originally set up, the oscillatory motion was not critically damped, and the small overexpansion of a portion of the gas resulted in the formation of a dense white fog, which completely filled the chamber after a few expansions, making it unusable. If the condensation centers formed by the overexpansion had disappeared before the next expansion, no difficulty would have been encountered, but this was not the case. No adequate explanation of this phenomenon has been given.

In order to increase the damping, and thus eliminate the large overshoot, the connecting tube was loosely packed with copper wool. The amount of wool did not seem to be particularly critical, but in the experiment only enough was used to eliminate the overexpansions; had too much been used, the expansion time would have increased, giving broad tracks which are difficult to measure. There is almost no background fog in the photographs of the chamber, and the chamber is sufficiently stable to need adjustment no more often than once daily.

Plates II, II', and IV are enlargements of cloud chamber pictures from the thirty-five-millimeter film. The plates show a track of minimum ionization, a proton, and a shower

#### P. Illumination and Photography

The chamber is photographed through a conical hole in the magnet core. The camera used for this experiment was especially constructed for the task and utilizes an ektar f-4.5 lens with a fifty-millimeter focal length. The rewind system is electrically operated, and the magazine has a capacity of 100 feet of thirty-five millimeter film. The framing arrangement permits 450 pictures to be taken on a 100-foot strip of film. Several types of film have been tried. The best results so far have been obtained with Eastman Linograph Ortho film. This film is exceptionally fast in the blue region and is not prohibitively grainy. Illumination is provided by four Sylvania type R-4340 photo-flash tubes operating at 2500 volts and having an energy dissipation of 100 watt-seconds each per flash. The energy is stored in a bank of thirty-two-microfarad condensers. Each flash tube is backed with an aluminum foil reflector and has a cylindrical collimating lens in front of it. This can be seen in Plate V, which shows the magnet face with the cloud chamber, geiger tubes, and flash tubes in position. The chamber is masked so that the illuminated depth is restricted to one inch.

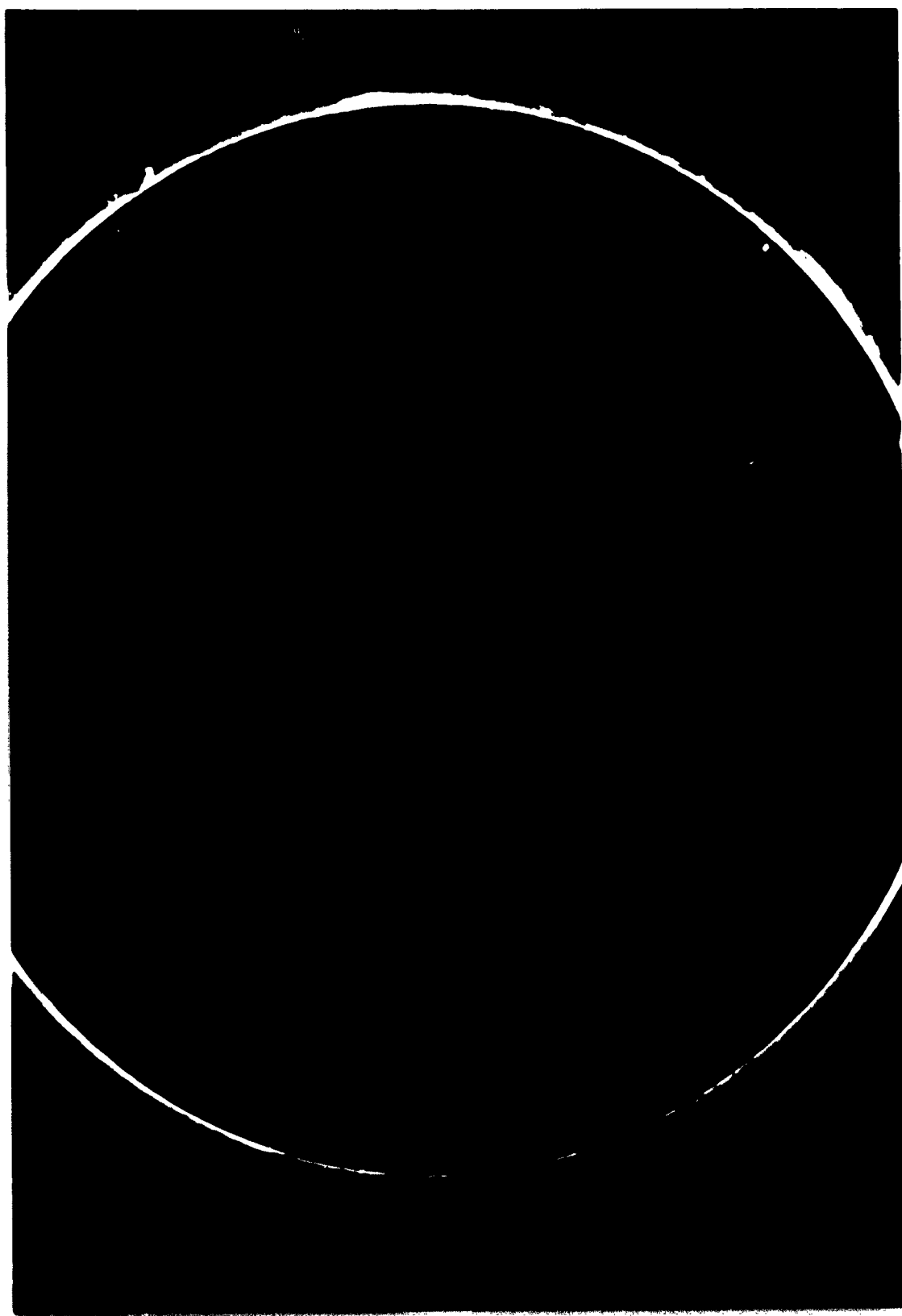


PLATE II. A MESON TRACK



PLATE III. A PROTON TRACK



PLATE IV. A SHOWER

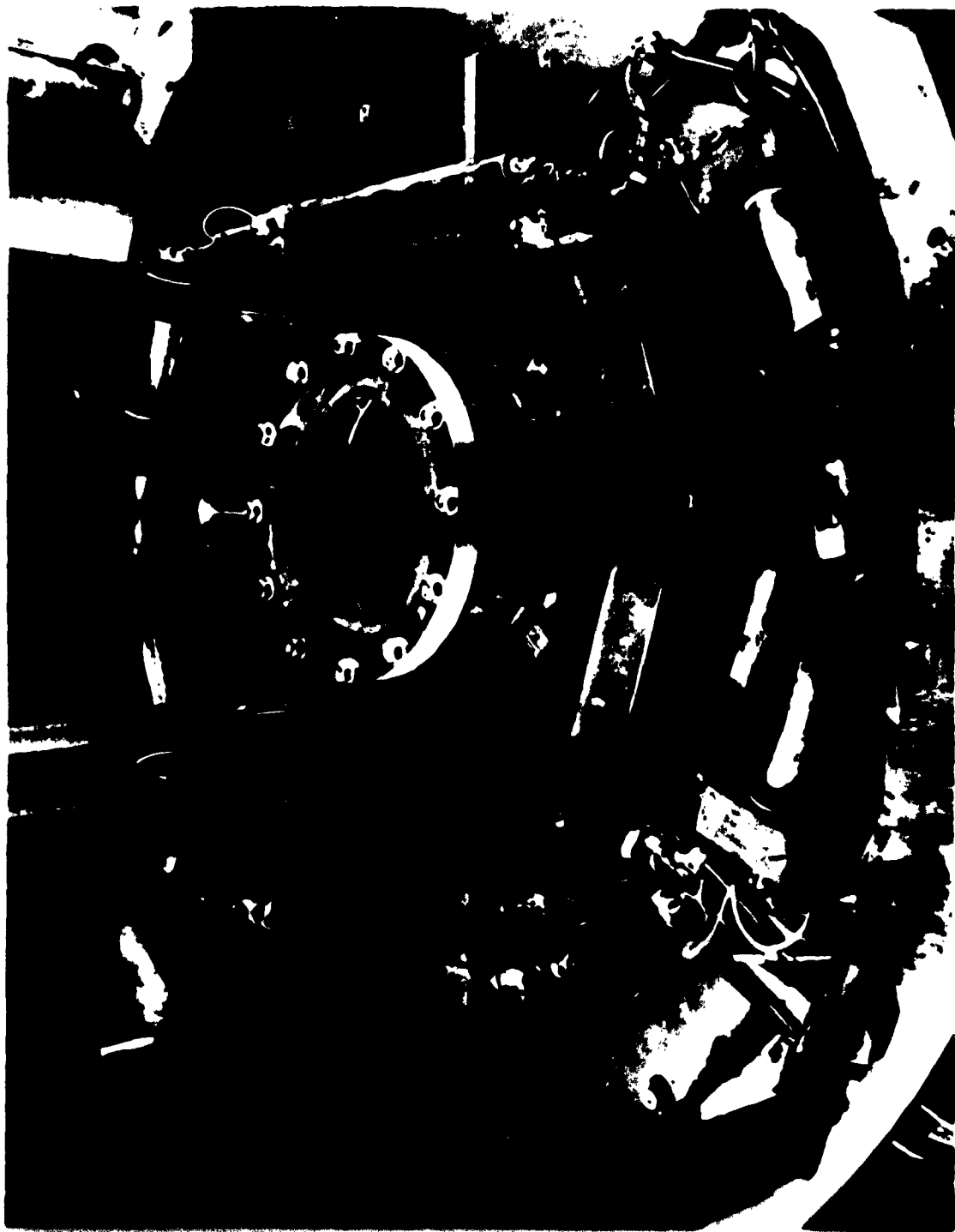


PLATE V. THE MAGNET FACE SHOWING THE CLOUD CHAMBER, THE FLASH TUBES, AND THE GEIGER COUNTERS

In many cloud chamber arrangements, stereoscopic viewing is essential. In experiments of this type, however, stereoscopic viewing is not so important. Here one depends upon the statistical analysis of a large number of tracks, and not upon the results of one or two unusual events. Stereoscopic viewing would be of help only in determining the angle the particle makes in traversing the chamber. The left-right angle is, of course, known, but the front-back angle is not. The maximum angle which a track may have is limited by the geiger counters. These are twelve inches apart and have a width of three-fourths inch. Thus, the maximum error in a momentum measurement due to this effect is of the order of 6 percent. The average error is considerably less.

#### C. Magnets and Cooling System

The magnet used in this experiment was originally intended for use in aircraft operation. This necessitated a compromise between economical operation and weight. Plate VI is a view of the magnet core and coil assembly prior to assembly in the housing. The magnet coils are wound of 0.23 x 0.80 inch copper buss and are contained in a steel housing, which also serves as the external portion of the magnetic circuit. The magnet weighs two thousand pounds, the weight being about equally divided between copper and steel. To achieve a field of 8200 gauss a current of 800 amperes, giving  $1.7 \times 10^5$  ampere turns, is required. The power dissipation is then 32 kw.





PLATE VI. THE MAGNET CORE

The cooling system utilizes forced feed of transformer oil. The oil-flow path has been restricted by a system of baffles so that there is an oil flow past all surfaces of the copper. The transformer oil is then cooled in an oil-water heat exchanger. An oil flow of about sixty gallons per minute is used. With this method of cooling, current densities of 7000 amperes per square inch of copper can be used continuously. To obtain a field of 8200 gauss, a current density of 4000 amperes per square inch of copper is necessary.

For stable operation of the cloud chamber it is necessary to maintain it at a constant temperature to about 0.1 degree centigrade. In order to achieve this regulation for long periods of time, the temperature control to 0.01 degree centigrade is required. Temperature control is achieved by maintaining the magnet assembly, with which the cloud chamber is in intimate thermal contact, at a constant temperature. With the present equipment the inlet oil temperature is measured by noting the change in the resistance of a copper coil placed in the oil stream. The change in the coil resistance upsets the balance in an a-c bridge which, when amplified by a Brown-type amplifier, drives a split-phase motor controlling a by-pass valve on the heat exchanger. The valve then either opens or closes in such a manner as to bring the bridge back into balance. This system provides temperature control of the inlet oil to 0.01 degree centigrade. The magnet temperature is indicated by a second Brown-type recording potentiometer suitably altered to measure the changes in resistance of a second

coil. Plate VII gives the circuit for the temperature-control system.

#### D. Uniformity of the Magnetic Field

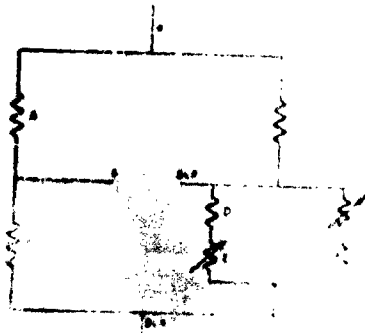
The magnetic field at the center of the gap was measured as a function of the energizing current by the use of a flip coil of known dimensions and a ballistic galvanometer. The galvanometer was calibrated by reversing a known current through a standard mutual inductance. It was found that the magnet began to saturate at rather low field values due to the small amount of ferromagnetic material used in the magnetic path. At about 8000 gauss saturation is nearly complete, and the slope of field versus energizing current is such that current stability to 3 percent will yield field stability of about 1 percent.

In exploring the field off center, a bismuth spiral was used. The spiral was calibrated in the center field of the magnet where the field had previously been measured in a basic manner. The field was investigated for considerable distances both axially and along a horizontal and vertical diameter. The field was found to be uniform to better than 1 percent over the entire illuminated volume of the chamber.

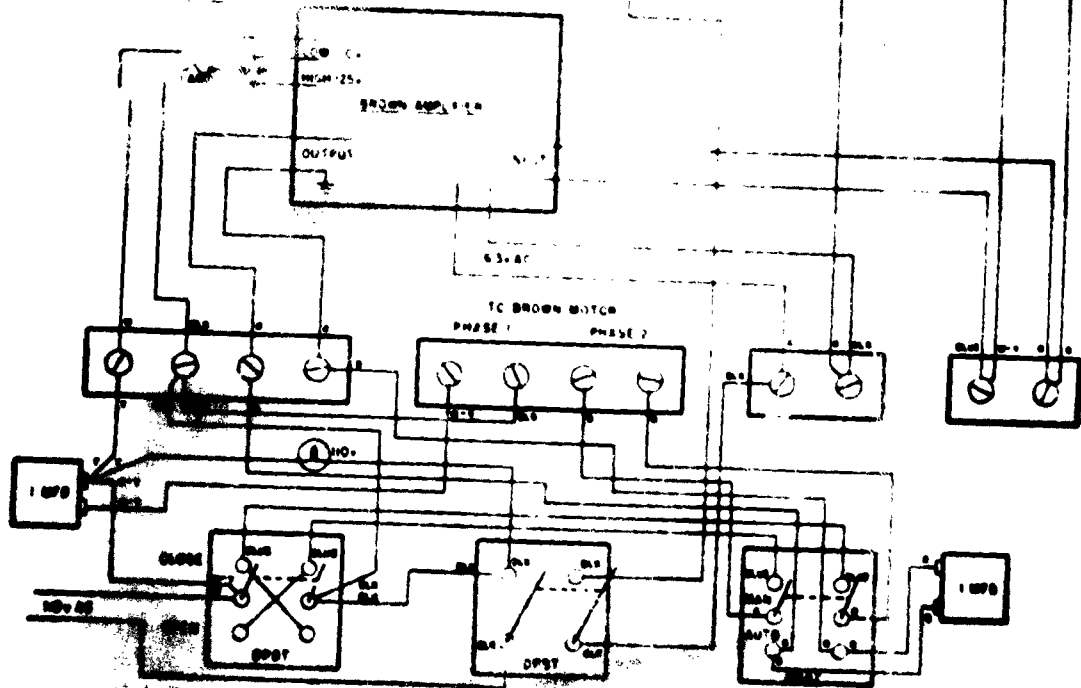
#### E. The D-C Magnet Supply

For the operation at Climax, Colorado, a motor-generator set was used to supply the current necessary to energize

# BRIS - SCHEMATIC



## TEMPERATURE CONTROL UNIT



the magnet. The generator has a capacity of 100 kilowatts and is a separately excited, compound wound machine. The generator control circuit is given in Plate VIII. The generator showed considerable fluctuations due to the large day-to-night temperature changes and had to be adjusted several times daily. The magnet current was recorded continuously, and only short time variations of as much as 1 percent occurred during the experiment.

#### F. Event Selection

The event selection system used in this experiment is considerably more complex than necessary, but the initial design was deliberately made quite flexible so that the unit could be used for many other experiments. It uses a threefold coincidence circuit of the Rossi type with a resolving time of 1.6 microseconds. Four anticoincidence inputs were provided so that it would be possible to count the cosmic ray background rate in the geiger tubes of the anticoincidence trays during a run. It has been found that up to four geiger tubes may be connected to one anticoincidence input and still allow for checking the operation of the geiger tubes by counting the cosmic ray background rate for a reasonable length of time. If more than four tubes are connected to a particular input, it is difficult to tell if one of the geiger tubes is counting too high or too low, since the effect is masked by the normal counting rate of the remaining tubes.

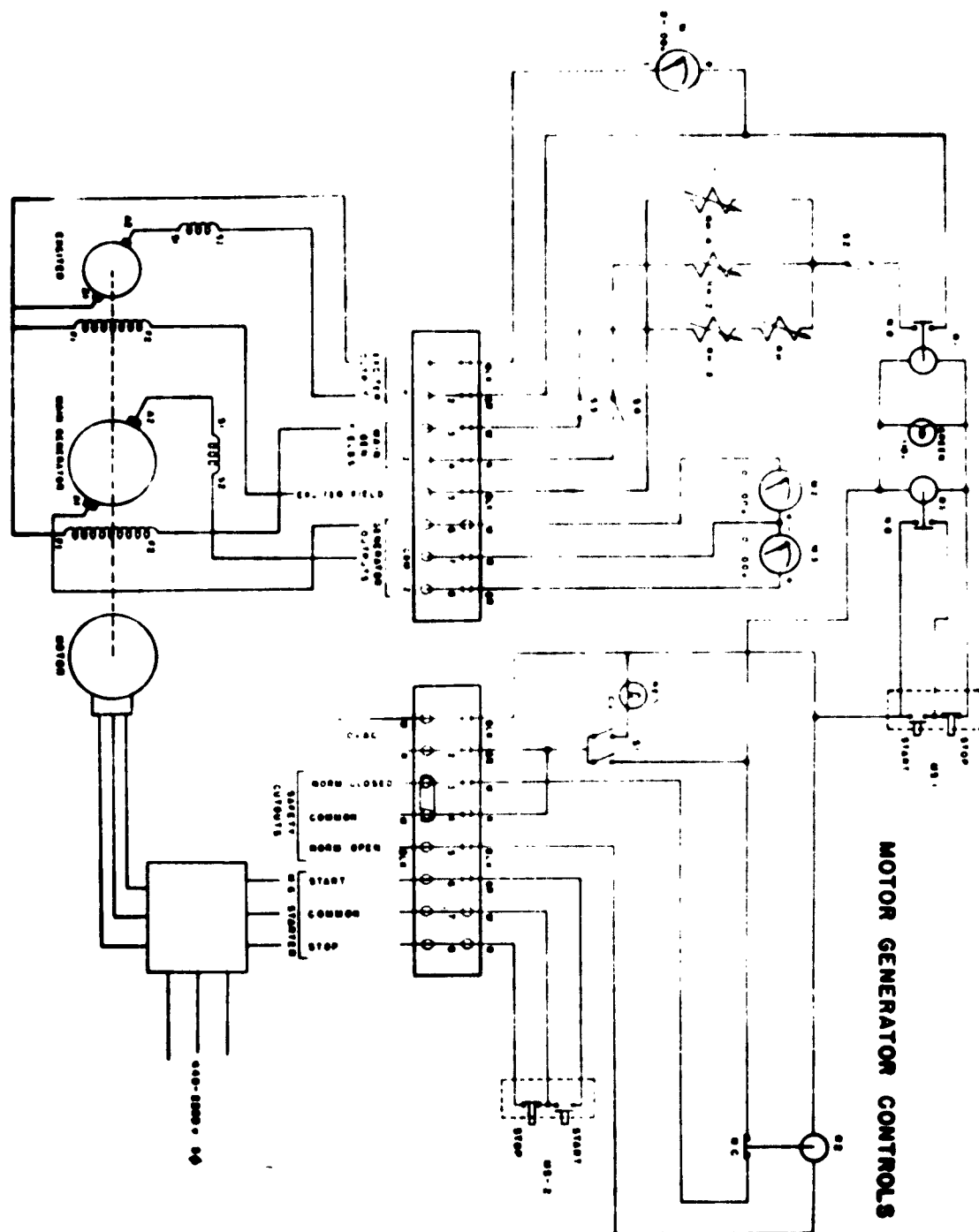
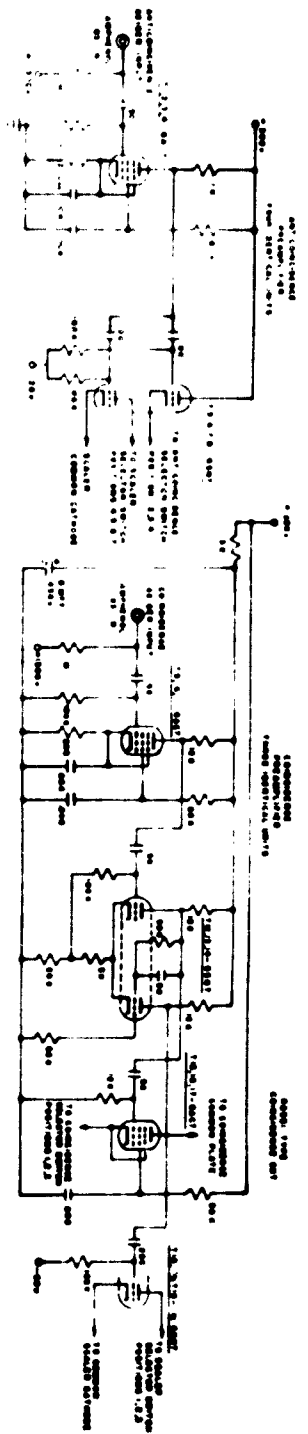


Plate IX shows the schematic diagram of the event selector. The upper left-hand corner shows the anticoincidence pre-amplifier. Four identical units are used. The upper middle section shows the coincidence pre-amplifier and the Rossi type coincidence tube. Three identical units are used. After amplification the anticoincidence pulses are received by the anticoincidence mixer and pulse shaper. After being properly shaped they are then fed to the anticoincidence blanking pulse generator, which generates a five-microsecond blanking pulse. Unlike a univibrator, this generator can be retriggered during a cycle, and hence there is no electronic dead time for pulse rejection. The coincidence pulse which was derived in the Rossi type coincidence circuit is then fed to the coincidence delay univibrator. This was done in order to insure positive blanking of the coincidence pulse in the anticoincidence mixer. The coincidence pulse is delayed here by two microseconds. Thus, in an event in which both the coincidence geiger tubes and the anticoincidence geiger tubes are actuated, the coincidence is recorded, and at the same time the blanking generator starts. The coincidence pulse is then presented to the mixer after a delay of two microseconds and lasts only 1.6 microseconds, insuring that the five microsecond blanking pulse has an overlap at both the first and last of the coincidence pulse. The actual "C-A" mixer is of the Rossi type. The pulse output cathode followers are shown at the bottom center of the schematic diagram. Switching details and power supply





connections are shown at the far right.

#### G. Cloud Chamber Control Unit

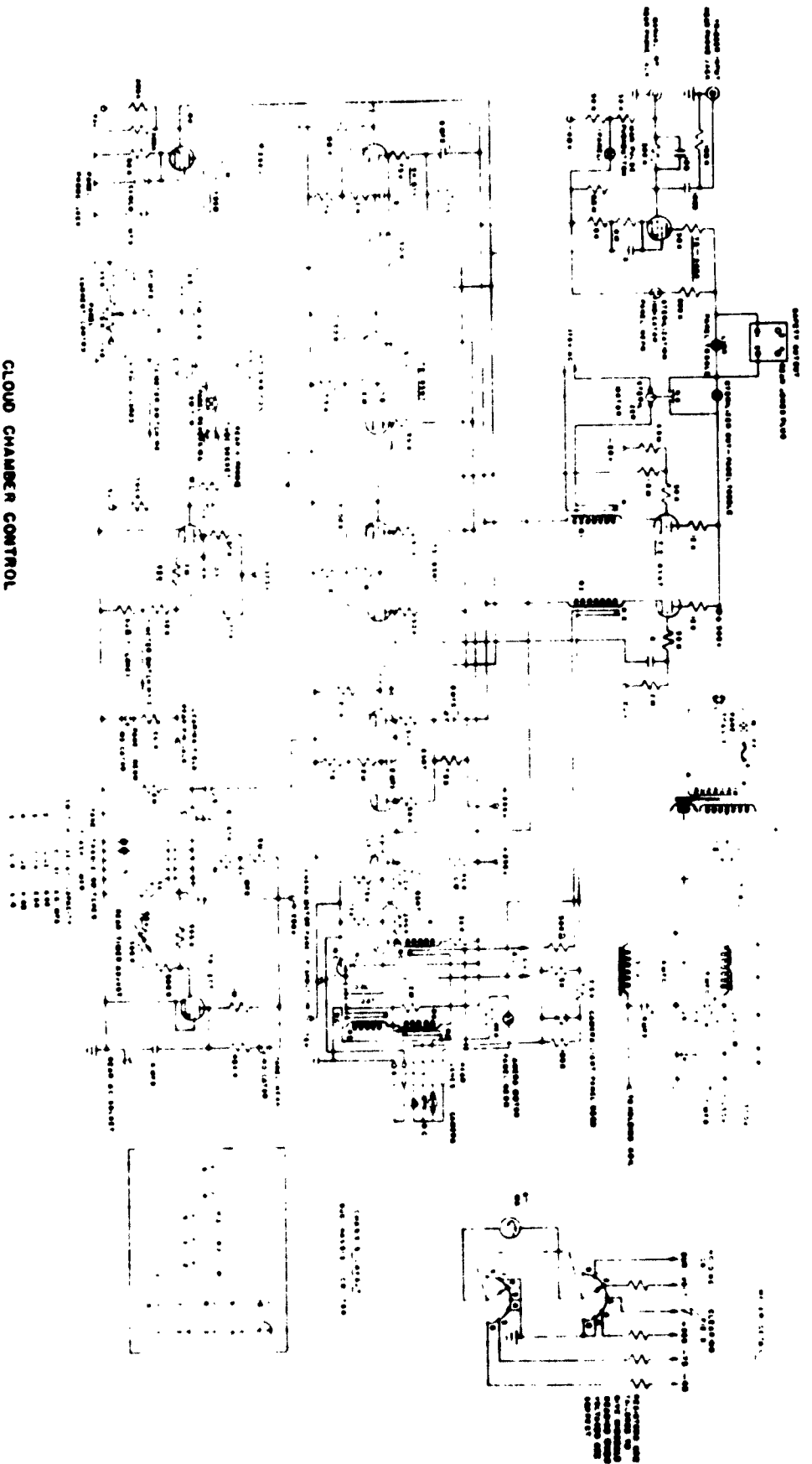
The cloud chamber control unit shown in Plate X must provide for the following functions:

1. Expand the chamber
2. Turn off the clearing field
3. Actuate the flash lamps
4. Rewind the camera
5. Record the expansion
6. Sterilize the unit so that no further expansion may take place until the cloud chamber has recovered
7. Provide for manually pulsing the chamber and provide for interlocks

The cloud chamber control circuit is of rather standard design. In order to properly sequence the cloud chamber, several timing delays are derived from timing univibrators. The input trigger thyatron, shown in the upper left-hand corner of the schematic diagram, delivers a positive pulse from its cathode which triggers all further operations of the cloud chamber control circuit. The first four tubes in the middle row of the schematic diagram are timing univibrators. Their time of operation is computable directly from the time constants involved. Thus, in the first stage, tube number four, a time constant of 0.5 microfarads times two megohms, or one second, produces a timing pulse of one-second duration. The

# CLOUD CHAMBER CONTROL

FIG. 1



second timing initiator for the camera and the third is a tenth-second, and the fourth is a hundredth-second. The other timing initiator is connected to a tube 11, appearing on the upper left half of the schematic diagram. This energizes a self-stabilizing timer responsible for the camera's self-stabilization time which is necessary to allow the chamber to come back to operating condition after an exposure.

Two other portions of the circuit are of interest, since they contain some unusual features. The camera motor rewind system, tube number eleven, appears on the center left of the schematic diagram. This circuit is essentially a square wave circuit, having two complex and rather complicated time-stable in time. Thus, the camera motor is energized and remains energized until it has wound over one frame. The complexity is necessary because of the fact that the camera motor is about ten times as slow when placed in the fringe field of the magnet, its normal position, as when allowed to run in essentially field-free space.

The photo-flash timer shown on the lower right of the schematic diagram is also of interest. Time delays from one hundredth of a second to thirty-two hundredths of a second can be achieved by the use of five toggle switches. These are arranged in binary fashion and the separate delays from them are additive. Thus, if a delay of eleven hundredths of a second is required, switch number one, two, and four are placed

in an operating position. The delays of one hundredths of a second, two hundredths of a second, and eight hundredths of a second are then additive. It is interesting to note that the capacity of the timing condensers in microfarads is equal to the time delay in seconds.

An auxiliary high voltage supply is provided for the operation of the photo-flash lamps. Since this supply is required to furnish 2500 volts from a bank of capacitors of 128 microfarads, it is an extremely dangerous unit, and special precautions are necessary to safeguard personnel. Interlocks and special connectors have been provided.

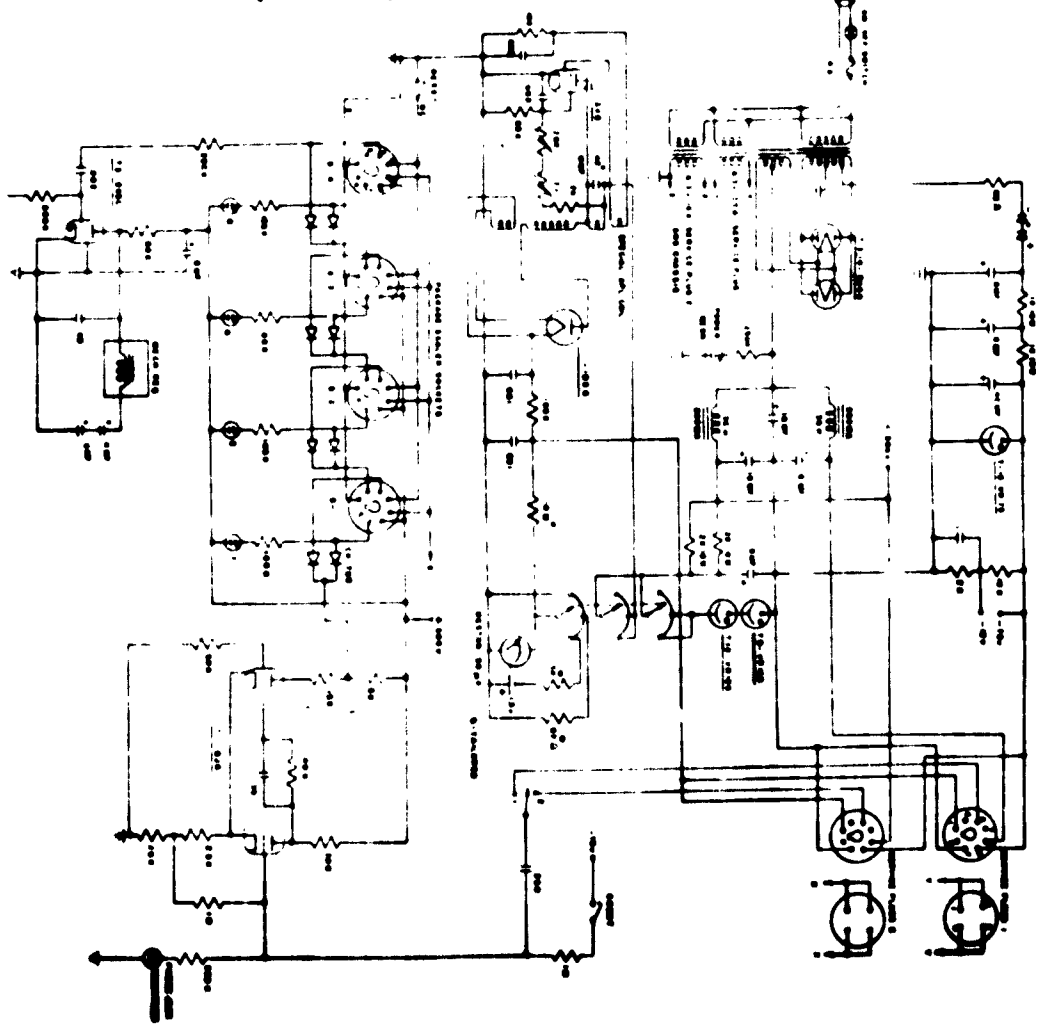
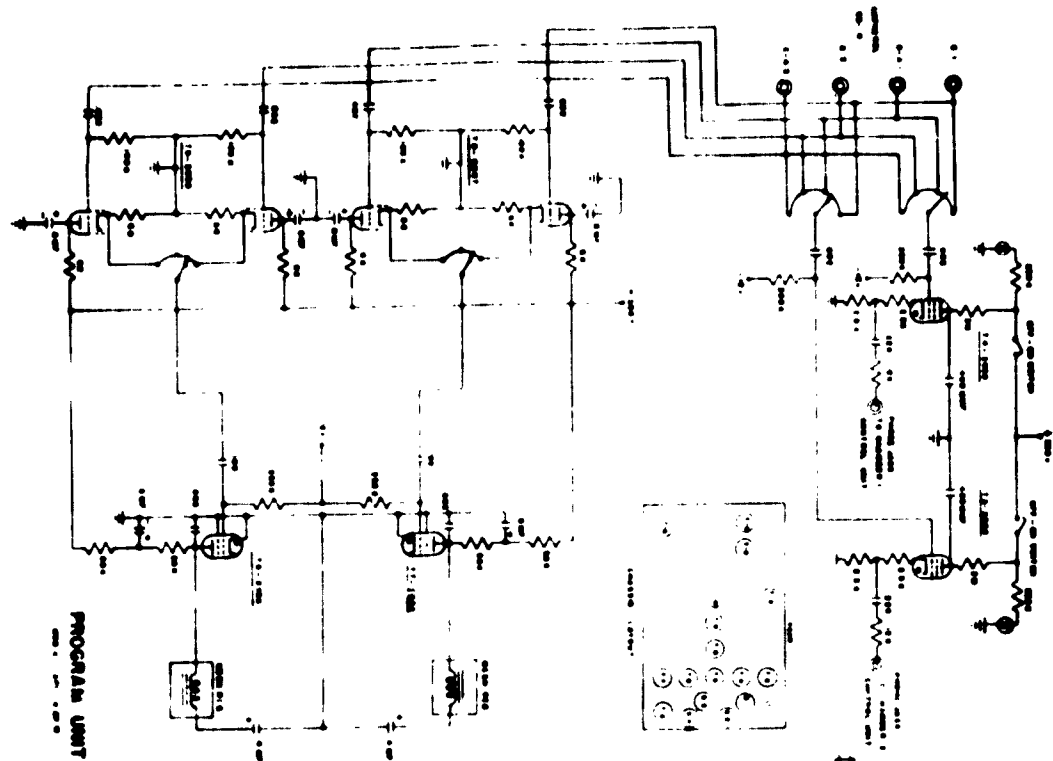
#### H. The Program Unit

Although only one cloud chamber and magnet were used in this investigation, there are actually two identical magnets and chambers mounted in a common frame. The electronic circuits were designed so that both units could be operated simultaneously, either on separate experiments or on one single experiment utilizing the two units together. This feature made necessary a program unit which could be used to interconnect the two units, if it seemed desirable.

In addition, there are three central facilities necessary for the operation of, and recording of data from, an event selector. In the interest of economy of space and materials, the program unit was designed to supply these facilities to both event selectors. The program unit schematic

diagram is given in Plate XI. The facilities supplied to the event selectors are: geiger counter voltage, a counting circuit for obtaining the background count, ray counting rate of the geiger tubes used, and mechanical registers for recording the number of coincidences and coincidence-minus-anticoincidence pulses received. Of these units, only the geiger counter voltage supply is of sufficient interest to warrant a detailed discussion.

The geiger counter voltage supply is of the radio-frequency type and uses a specially constructed coil. This coil has a secondary winding which consists of six separate "pies." This is necessary because of the relatively high radio-frequency voltages appearing across this coil. Also, the filament voltage for the high voltage rectifier comes from this coil. The maximum geiger voltage obtainable has been limited so that the geiger tubes will not be damaged, should the supply accidentally be turned too high. Without such limiting, a maximum voltage of 1600 volts can be obtained. The limiting voltage is 1425 volts. The meter used for determining the voltage has a differential scale in addition to a 0-2500 volt scale. This scale goes from one thousand volts to fifteen hundred volts and permits the geiger tube voltage to be set within five volts. Such a scheme is invaluable when measuring the plateau of the geiger tubes. In order to protect personnel, the geiger supply has a maximum current output of less than ten milliamperes, which is a factor of two less than

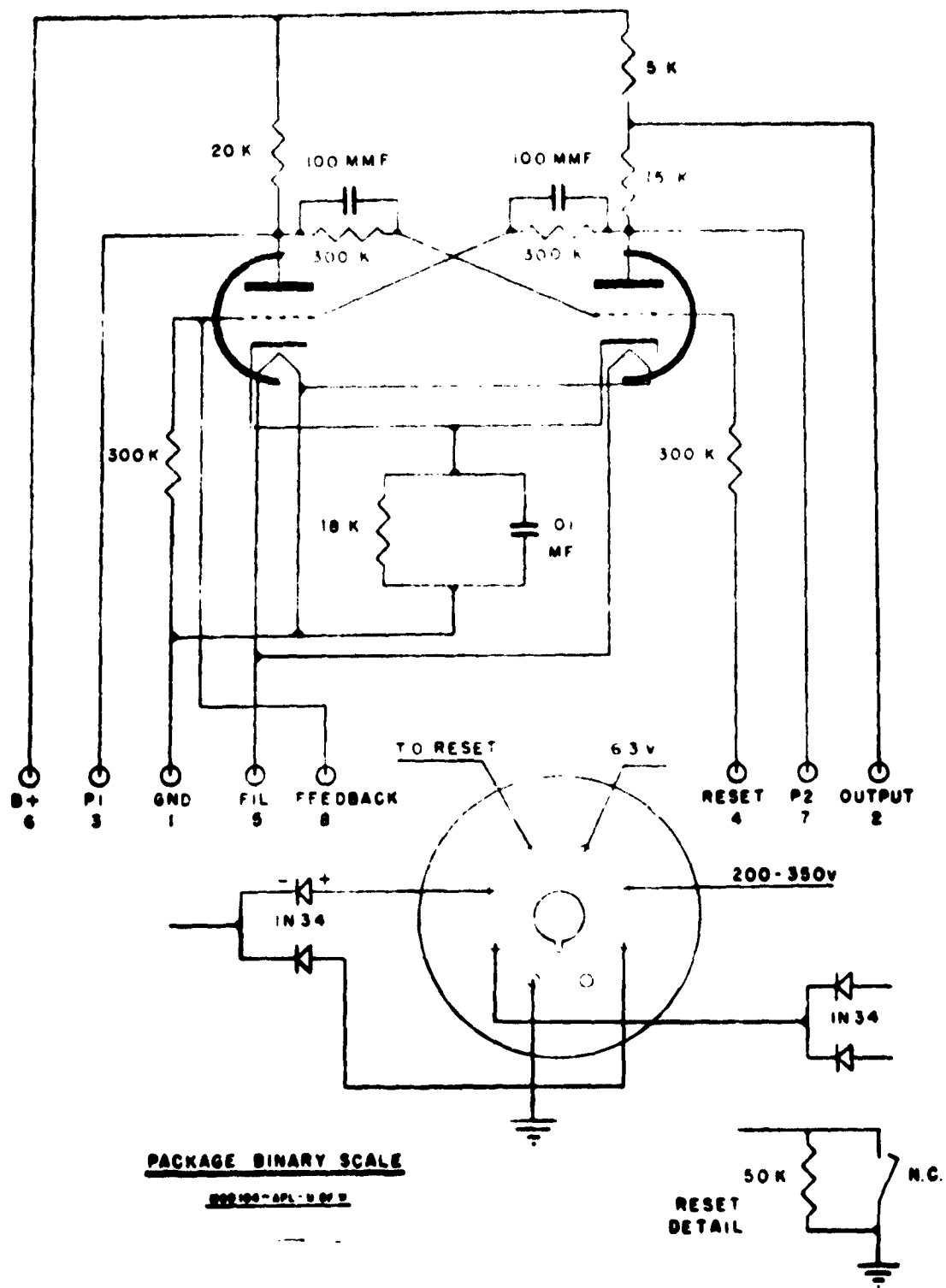


"let go" current, and a factor of three less than lethal current. This is possible because the geiger tubes require very little current.

The binary scales used in the program unit are of special design. Their circuit is given in Plate XII. As can be seen, these are packaged binary scale systems, and they are constructed on an octal socket base. These scales are extremely stable, and thus far have given no trouble. So far as is known, these scales are the only binary scales which can be constructed without the necessity of a tailoring process.

### I. The Geiger Counters

The geiger tubes used in this investigation are of ordinary glass-envelope construction with a cathode of copper tube and an anode of five-mil tungsten. They were constructed by this laboratory for use in these experiments. The cathode is six inches long and has a diameter of three-fourths of an inch. This gives an effective area of thirty square centimeters. The tubes are filled with a mixture of 90 percent argon and 10 percent petroleum ether by volume to a pressure sufficient to bring the onset of counting at about 1180 volts, and a plateau center of about 1300 volts. No measurements of tube life have been made, but it has been found that the tubes need refilling after about  $10^9$  counts. The plateau is about 300 volts long with a slope of less than 5 percent.





### III. THE EXPERIMENT

#### A. Location and Transportation

This investigation was carried out in the fall of 1948, the expedition leaving Seattle August 3. To transport the apparatus a large radar truck and trailer was obtained from the Navy, and the main equipment was mounted on it. The auxiliary equipment, including a large squad tent for storage of equipment, and equipment for camping were transported on a 1-1/2-ton Dodge truck. Power generating equipment was transported on a 2-1/2-ton GMC. A gas trailer and tanker to be used for transporting and storing gasoline and diesel oil for the generator was also taken, along with two other vehicles, a 1/2-ton Dodge pickup and a jeep for use in transporting small supplies and personnel. This transportation equipment can be seen in Plate XIII.

Although considerable preliminary investigation with the cooperation of the United States Forest Service had limited the number of possible locations, the final decision as to the location was not made until a thorough investigation by the members of the expedition could be made of such places as Independence Pass (elevation 12,280 feet). It was finally decided to locate on Fremont Pass, Climax, Colorado, at an elevation of 11,380 feet. Although not as high as Independence Pass, the Climax Molybdenum Company, located on the pass, offered to supply the necessary power and water in ample



PLATE XIII. THE EXPEDITION BEFORE LEAVING SEATTLE

quantities and, in addition, provided living accommodations at the hotel used by the bachelor miners. They also offered the use of the machine shops, should extensive repairs be necessary.

About a week was required to set up the equipment and provide space in the tent for routine checks and repairs on the instrumentation. The Climax Molybdenum Company was extremely helpful in getting the electrical and plumbing work done quickly so that we could get into operation without delay. Power was supplied from a 440-volt three-phase transformer bank, and the water supply was obtained from the main mill water line. Since the water supply had a large positive head, it was unnecessary to use pumps to circulate the water through the heat exchanger. Plate XIV is a view of the location, and Plate XV is a view of the radar truck showing the magnets and other equipment.

#### B. Experimental Procedure

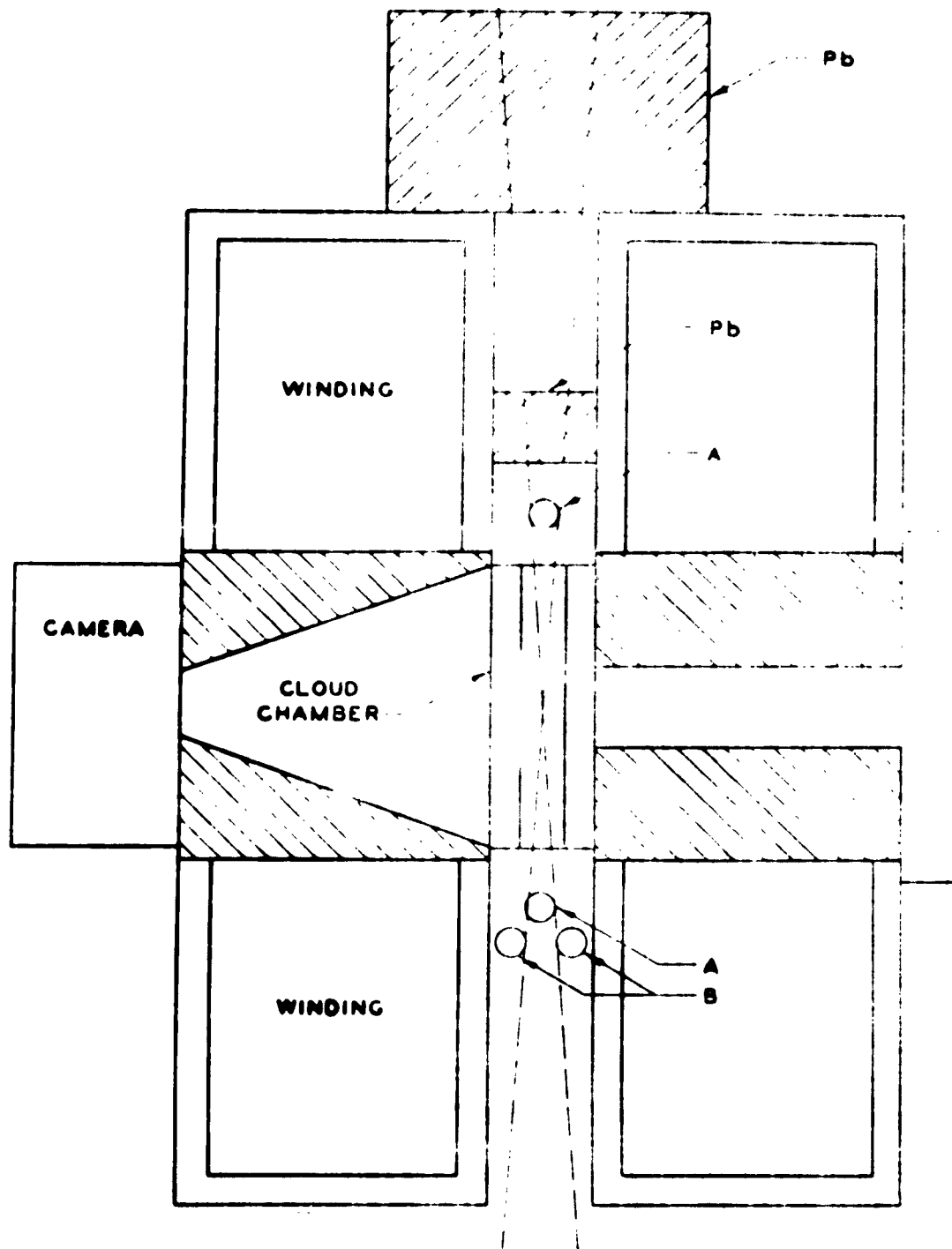
The ultimate aim of the expedition was to measure the momentum spectrum of the cosmic radiation at altitude under various thicknesses of absorber. The experimental arrangement used is shown in Plate XVI. Geiger counters were placed above and below the chamber, defining a cone of about one-thirtieth steradian solid angle and having an area of thirty square centimeters. The geiger counters were arranged so that none of the magnet was included in this solid angle. The coincidence counters are shown at position "A." Anticoincidence



PLATE XIV. THE LOCATION ON FREMONT PASS



PLATE XV. THE EQUIPMENT IN THE RADAR TRUCK



**SCHEMATIC DIAGRAM OF THE MAGNET,  
CLOUD CHAMBER, COUNTERS AND ABSORBERS**

counters are shown at position "B" and were used through about half of the experiment in order to eliminate shower events. The various thicknesses of lead absorber were placed above the upper trigger counter, the five-centimeter block being directly above the upper coincidence counter, and an additional fifteen centimeters being located above the entire assembly.

The coincidence counting rates with field on and field off are given in Table I for the three experimental arrangements used.

TABLE I

Coincidence Counting Rates in counts/second

Field	No absorber	5 cm lead	20 cm lead
off	0.045	0.030	0.023
on	0.034	0.028	0.023

The ratio of 2:1 of the no-absorber rate to the 20-cm-lead rate (with the field off) is just the ratio of the total to the hard component at this altitude given by Rossi. The agreement must be in part fortuitous, since the two-counter telescope used was hardly adequate for a reliable rate determination. With no absorber above the telescope the field shows a strong effect in reducing the counting rate from 0.045 to 0.034 counts per second. This reduction corresponds to the large numbers of low energy electrons whose momenta lie below

the magnetic cutoff of the equipment used. As explained later, this cutoff comes at a momentum of fifty Mev/c. In the case of twenty centimeters of lead above the chamber, the magnetic field has no measurable effect, indicating that the radiation passing through the 20-cm lead block does not contain many low momenta particles. This is in accord with the established notion that passage through an absorber tends to "harden" the radiation. Actually what happens is that the electrons are removed by cascade showers and the resulting mesons are quite penetrating, hence, although the meson energy has decreased slightly, the absence of the electrons gives a net effect of making the radiation more penetrating.

### C. Data Taking

After the equipment was thoroughly checked, seven rolls of film (450 frames per roll) were taken with no absorber above the chamber, and with the magnetic field at 10,000 gauss. After examination of the photographs, it was seen that the chamber had considerable turbulence along its periphery. The field was reduced to 8200 gauss, and turbulence effects were found to be negligible. The remaining thirty-two rolls of film were taken at this reduced field strength. Fourteen rolls were taken with no absorber above the chamber, eleven with five centimeters of lead above the chamber, and only seven with twenty centimeters of lead above the chamber. Throughout the experiment the magnetic field was occasionally changed in



direction so that any asymmetry in the radiation brought about by the field could be checked. Data also were taken with and without the anticoincidence circuit to check its effect.

No real difficulties were encountered except for a two-day dust storm and the inevitable snow near the end of the stay at Climax. The final thirty-two rolls of film were exposed in the thirty-two days from October 5 to November 5.

#### IV. MEASUREMENT OF TRACK CURVATURES

Several methods of measuring track curvatures have been used by various investigators. A method employed by Anderson (4) using a traveling microscope in which the coordinates at various points along the arc are measured and used to compute the curvature is quite time consuming, and not particularly adapted to the measurement of a large number of tracks, such as one obtains in the measurement of the momentum spectrum. An optical method, due originally to Blackett (5), although capable of yielding quite precise measurements of track curvatures, is not useful with curvatures of small radii, and, hence, is unusable for the lower momenta obtained in this investigation. In the interest of simplicity, but at the expense of decreased resolution at the high momentum end of the spectrum, a comparison method was chosen for measuring the track curvatures in this experiment.

In order to compare the cloud chamber track with a standard arc, a machinist's bench comparator was altered so that the 35-mm photograph could be projected on the ground glass screen. Plate XVIII is a picture of the comparator as altered for this use. A film carriage was provided for the comparator as well as a means for moving the film holder so that the projected track could be rotated to a horizontal position on the screen. The entire optical system was such that the projected image was the size of the cloud chamber.



PLATE XVII. THE COMPARATOR

The standard arcs used as the basis for comparison were scribed full size on plate glass coated with Amalgam. The scribing system was of the Evans linkage type which generates arcs of ellipses. The linkage system is shown in Plate XVIII. For the short length of arc used (about fifteen centimeters and a minimum radius of curvature of thirty centimeters) the approximation of the elliptical arc to that of a circle is good to within 1 percent. For each radius of curvature two arcs were scribed, separated by a distance of 0.7 millimeters. In this way the track whose curvature was to be measured could be centered between the two arcs, and hence could be seen along its entire length. If only one arc is used, it is difficult to observe the closeness of fit unless the arc is placed over the track to be measured, and then, of course, the track cannot be seen.

Twenty-four standard arcs were used in this analysis, ranging from 0.3 to 10 meters radius. The radial increment between successive arcs was not constant, but increased in an exponential fashion except at the smallest radii of curvature. Since the curvature of a track can be either very close to one of the standard arcs, or can lie in between any two of them, there are forty-nine possibilities for a particular measurement. The curvature and its sign were recorded for all tracks meeting selection criteria described elsewhere.

In order to make the measurements independent of the optical enlargement, comparison arcs were prepared from the

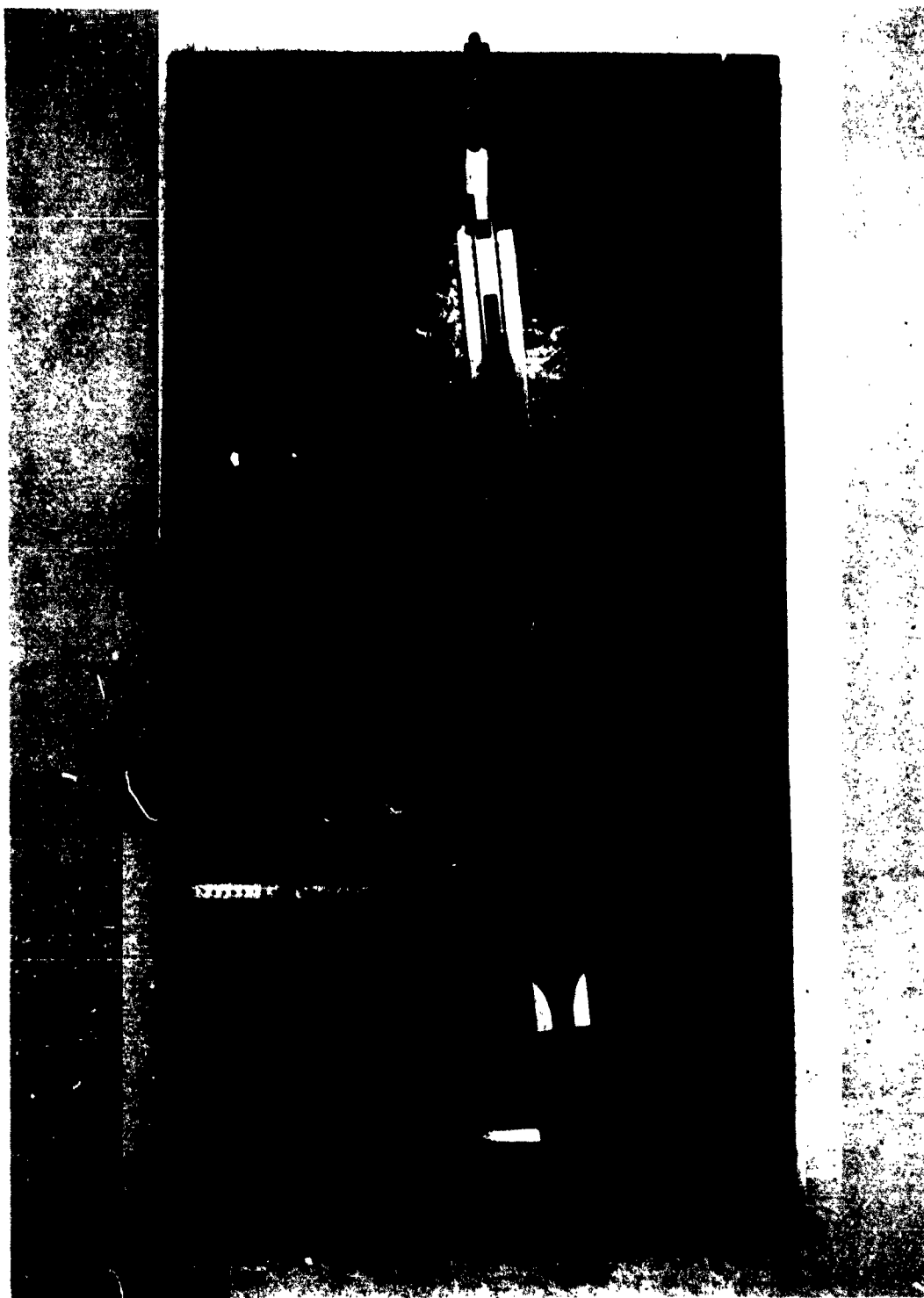


PLATE XVIII. THE EVANS LINKAGE SYSTEM

standard curves through the sequence of operations followed in obtaining the projected image of a cloud-chamber track. Thus, the standard arcs were first photographed under conditions prevailing when photographing the chamber. The resulting 35-mm negative was then projected in the comparator, exposing a photographic plate placed in the position normally occupied by the ground glass screen. Since the sequence of optical operations had been the same for the comparison curves and the cloud chamber photographs, no further information regarding the optical system was necessary for a track located in the center of the chamber and having a positive curvature.

Each step in the process outlined above was thoroughly checked so that systematic error could be avoided. Several of the standard arcs scribed on the Aquadag-coated plate glass were examined by means of a traveling microscope to insure that the Evans linkage system was operating properly. Also, the optical system was examined to be sure that a straight line remained a straight line and that there would be no difference in the measured value of a track if it were turned over so that it had a negative curvature rather than a positive one.

In order to check the consistency of the measurements a group of several hundred tracks were measured by several different observers. The individual results were then plotted against each other as abscissa and ordinate. For perfect consistency all points should have been on a line of slope one passing through the origin. In the actual plot a symmetric

distribution about this line was obtained, which indicated a consistency of better than 10 percent for curvatures less than about three and a half meters, becoming progressively worse at higher values, until at ten meters the error was of the order of three meters.

The radius of curvature of a particle is related to its momentum by:

$$p = 300 B r,$$

where  $p$  is the momentum in electron volts divided by the velocity of light,  $B$  is the magnetic induction in gauss, and  $r$  is the radius of curvature in centimeters. The field strength used in this investigation was 8200 gauss, and hence a curvature of one meter may be taken as corresponding to a momentum of 250 Mev/c.

## V. SELECTION OF TRACKS FOR CURVATURE MEASUREMENT

In order to eliminate the soft component from the momentum spectrum as nearly as possible, only those tracks which occurred singly in the chamber were used. Tracks which were accompanied by obviously post-expansion or pre-expansion tracks, however, were not excluded. A few singly occurring tracks were not at such an angle as to definitely indicate counter control. Such tracks were not included. The fact that very few such tracks occurred indicates that the majority of tracks were counter controlled and, because of the geometry of the system, could not have originated in the chamber wall or surrounding material.

About 60 percent of all pictures taken showed singly occurring tracks. Because of the large number of tracks available, only the longest (fifteen centimeters out of a possible seventeen centimeters) were chosen for measurement. About 70 percent of all singly occurring tracks were this long or longer. Thus only tracks long enough for good curvature measurement were used, and those passing close to the chamber and subject to large turbulence distortion were avoided.

The subgroup of particles thus selected should not be different from the total body of data, and tracks measured form a distribution representative of the non-electronic radiation. In most air showers not more than one electron would be expected to be incident on the small cross-section of the



chamber (thirty-five square centimeters). However, the chamber wall and the upper geiger counter constitute only a small fraction of a radiation length (the distance in which a very fast electron loses a fraction  $(1 - e^{-1})$  of its energy by radiation), and an electron will not in general initiate an electron shower in passing through them. Thus, with no absorber above the chamber, large numbers of singly occurring low energy electrons will be included. On the other hand, with five centimeters of lead above the chamber, electrons of energy sufficient to penetrate the absorber have a high probability of initiating a cascade shower and will be recognized by the multiplicity of particles occurring in the chamber. This is clearly shown to be the case from the resulting data.

One further precaution was taken. It sometimes happened that at the end of usability of a particular chamber filling the chamber would go out of adjustment slightly between observations, giving rise to tracks which were not sufficiently dense to measure easily. In this case either the whole roll of data was rejected, or, if the number of tracks thus affected was not large, a complete block of exposures including all those of doubtful quality was eliminated. In no case were single frames discarded.

## VI. THE MAGNETIC CUTOFF

The twofold coincidence triggering arrangement with counters above and below the chamber has the effect of discriminating against low momentum particles. Below the minimum momentum a particle will be so severely curved that no matter what the position of entrance, or the angle made with the vertical, the particle will not be able to enter the lower geiger counter. In order to estimate the effect of the magnetic cutoff and obtain the magnitude of the effect for particles having momenta higher than the minimum momentum required, this effect was computed. A graphical method of computation was used which took into account the length criterion of track selection as well as the counter geometry used. In the computation it was assumed that the magnetic field extended to the counters in full strength. Actually, in the two inches between the counters and the chamber the field decreases quite rapidly. It was further assumed that the distribution in zenith angle obeys a  $(\cosine)^2$  law. A decrease of intensity with zenith angle less than  $(\cosine)^2$  would result in a smaller effect for the magnetic cutoff above the minimum momentum, while a more rapid decrease in intensity with zenith angle would give a larger effect. The latter case, however, has a small probability for the relatively low momenta considered in the computation.

The results of the computation show a complete cutoff at 50 Mev/c. The transmission rises rapidly, so that at 100 Mev/c the decrease in intensity is only 10 percent, and at 150 Mev/c the attenuation is negligible. The momentum spectrum found with no absorber above the chamber, in which many low energy electrons are present, shows the effect of the magnetic cutoff at the predicted momentum and constitutes experimental verification of the analysis. Within the statistical uncertainties involved in determining momentum spectra, the observed intensity above 100 Mev/c is considered to be unaffected by the magnetic cutoff.

## VIII. NORMALIZATION OF DATA

In the study of cosmic ray phenomena the absolute intensities of the various components of the radiation play a role of prime importance. The absolute intensity of a particular component is usually given as the flux of particles of that component in particles per second passing through a surface of one square centimeter per steradian for an infinitesimal solid angle. The data of an experiment are usually converted to absolute units by computing a normalizing factor for the experimental arrangement and then multiplying the counting rates by this normalization factor to arrive at intensities in absolute units.

The dimensions of the rate-determining elements used in this experiment are as follows:

Area of geiger counters                      30 sq cm

Mean distance between counters              30 cm

Thus the area is thirty square centimeters, and the solid angle included is one-thirtieth steradian. The normalization factor for the equipment is then about one  $(\text{steradian cm}^2)^{-1}$ . Since the estimation of the effective area of a geiger counter is subject to errors involving the end effect and also the mean path length of a particle through the counter which contributes to its efficiency, a direct measurement of the effective area of a small counter is difficult. Thus a second normalization method was explored. Since the coincidence

telescope used in this investigation had only two elements, the counting rates obtained with it cannot be compared directly with published data on the hard component intensity at this altitude. This is true because a twofold coincidence train is not at all effective for rejecting showers, especially at high altitudes.

From an analysis of the yield it has been established that 57 percent of the pictures taken with twenty centimeters of lead absorber above the chamber were of singly occurring particles. Thus, 57 percent of the counting rate of the coincidence telescope under twenty centimeters of lead corresponds to the counting rate of the hard component when filtered through  $232 \text{ gm/cm}^2$  of lead. By definition, the hard component is that radiation which has passed through  $167 \text{ gm/cm}^2$  of lead. In order to compare the counting rate obtained under twenty centimeters of lead with the established intensity of the hard component, it is necessary to consider the correction imposed by the additional absorber used in this experiment. The additional sixty-five  $\text{gm/cm}^2$  of lead is equivalent of about forty-two  $\text{gm/cm}^2$  of air. The altitude of Climax, Colorado, is 3.4 kilometers, and the atmospheric depth is  $680 \text{ gm/cm}^2$ . The additional five centimeters of lead used, then, should be equivalent to forty-two  $\text{gm/cm}^2$  of air, giving an atmospheric depth equivalent to  $720 \text{ gm/cm}^2$ . The counting rate at this atmospheric depth for the hard component is given by Rossi as  $1.22 \times 10^{-2}$  counts per second steradian<sup>-1</sup> cm<sup>-2</sup>. The

results of this experiment, when corrected for a fifty-seven percent yield show a counting rate of  $1.3 \times 10^{-2}$  counts per second. The normalization factor thus obtained is  $.94 \text{ ster}^{-1} \text{ cm}^{-2}$ . The normalization obtained when using the data for five centimeters of lead gives very nearly the same result, but because of the larger correction necessary to convert the figure to an equivalent absorber of  $167 \text{ gm/cm}^2$  is not considered to be as accurate as for the twenty-centimeter data. Since statistical uncertainties in the computation are of the order of 5 percent, the normalization factor may be considered to be unity. This value has been used in computing the spectra of this investigation.

## VIII RESULTS

## A. A Method of Tabulation and Plotting

The experimental procedure, measurement of tracks, and the criteria for track selection have been given. Of the total number of exposures, only about 4500 were of sufficiently good quality for measurement. Three thousand of these satisfied all of the requirements cited earlier, these being equally divided between the no-absorber case and the case of a five-centimeter lead absorber. The measured values of the tracks for a particular case were grouped according to the sign of the charge of the particle producing the track. This was not simply the sign of the curvature as viewed in the comparator since the magnetic field was reversed several times during the course of the runs to check on possible asymmetries caused by the field. The sign of the particles, as deduced by the direction of the magnetic field, was checked by an inspection of the signs of the particles producing an ionization density well above minimum and having a momentum commensurate with that of a proton with such an ionization density. Such tracks, as will be seen later, can be attributed entirely to protons, and hence have only a positive sign.

In plotting the data for a differential momentum spectrum the intensity is given in terms of particles per unit of momentum, or, if normalized to absolute units, the intensity is given in terms of the flux of particles per unit area, per

unit time per unit solid angle per unit of momentum. Mechanically the computation is made by dividing the number of particles in some momentum interval by the magnitude of the interval expressed in terms of the unit of momentum chosen, and then multiplying by an appropriate normalizing factor which takes into account the counting rate of the event studied, the number of pictures examined and the dimensions of the event-selecting part of the apparatus. The data of this investigation were obtained in terms of radius of curvature instead of momentum, and hence the following equation gives the intensity:

$$I_r = \frac{F N}{r}$$

where  $r$  is the radius increment in meters,  $N$  the number of particles in the interval, and  $F$  the normalizing factor. In all cases the normalizing factor has been computed to give the intensity in particles  $\text{sec}^{-1} \text{ster}^{-1} \text{cm}^{-2} (\text{Bev}/c)^{-1}$ .

Many methods of plotting the data have been tried, the most successful one being a simple, non-overlapping plot. The statistical uncertainty at each point is kept small by choosing a rather large interval containing in the order of 100 particles. In order to keep the statistics fairly uniform in terms of their percentage variation, no attempt has been made to take equal intervals of momentum. The uncertainties shown in the plotted points of the spectra are the statistical uncertainties and do not reflect the other sources of error, such as the uncertainty in momentum measurement.



As indicated earlier, there are a total of forty-nine intervals into which a particular measurement may fall, not counting the sign. A curvature was recorded as being equal to the curvature of a standard arc, if, when compared with the set of standard arcs, it was judged to be closer to that arc than the mean between that arc and the next. The tabulation of results then consists of counting the number of particles of a given sign judged to have curvatures falling in each of the forty-nine categories. Since the particles grouped in a division corresponding to a standard arc (hence not judged as lying between two standard arcs) are about evenly distributed about the value of the standard arc, it is assumed that half lie above the value and half below. This concept is important only at the value of ten meters, and in tabulations concerning particles of momentum greater than 2.5 Bev/c (ten meters radius of curvature) half of those particles included in the ten-meter group of the actual tabulation will be considered to be greater than ten meters. The tabulation of the actual data is given in Table II for both the no absorber case and the five-centimeter-lead-absorber case.

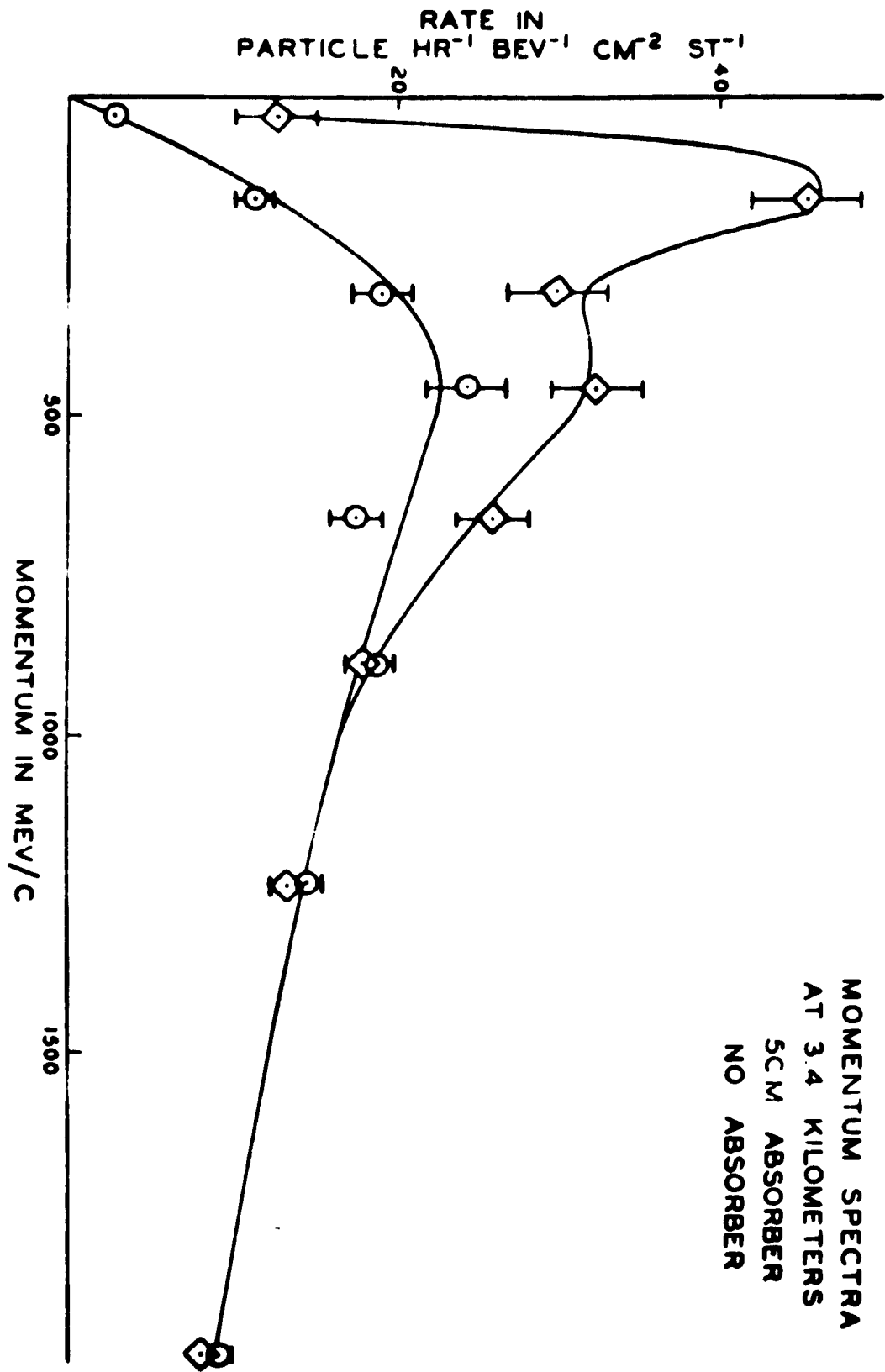
#### B. The Momentum Distribution

With no absorber over the chamber, a total of 1541 tracks were measured, 1064 having a momentum of 2.5 Bev/c or less. Including all tracks whose sign could be determined, there are 767 positive particles and 543 negative particles.

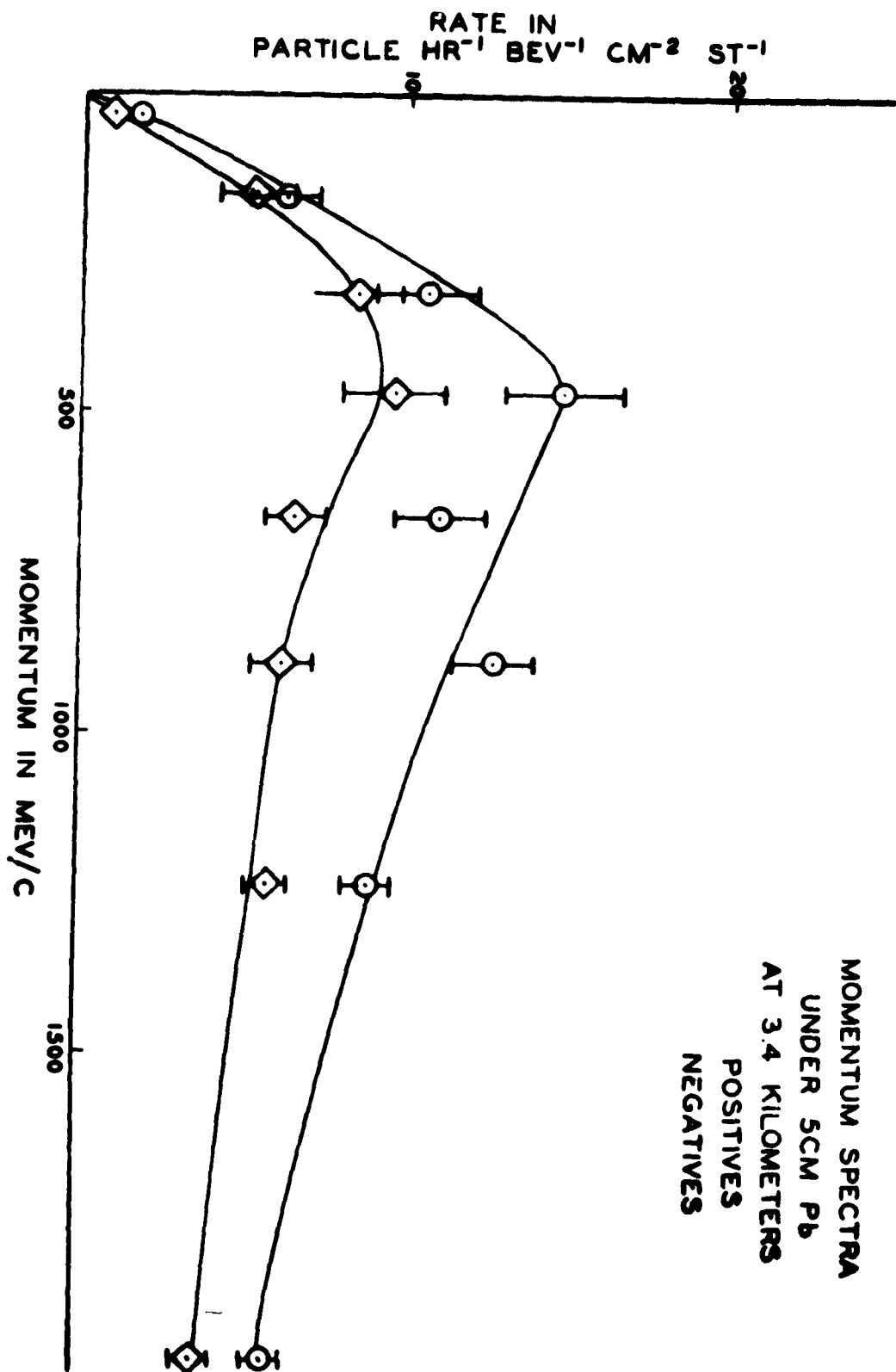
However, large numbers of electrons have been included in this case, and the ratio of positive to negative particles has little significance because of the dilution by the electronic component. A plot of the total field of data, including particles of both signs, is given in Plate XIX. The data for the no-absorber spectrum are given in Table III. The normalization factor computed for this case is  $0.163 \text{ ster}^{-1} \text{ cm}^{-2}$ .

With five centimeters of lead above the chamber a total of 1494 tracks were measured, of which 943 tracks correspond to particles having a momentum of 2.5 Bev/c or less. The positive excess for this case is  $1.5 \pm 0.1$  for particles lying in the momentum interval fifty Mev/c to 2.5 Bev/c. The positive excess for all particles, including those with momenta greater than 2.5 Bev/c, is the same within statistics. Since the distribution of positives and negatives is of interest, the two were plotted together on the same graph and are given in Plate XX. A plot of both positives and negatives is given in Plate XIX where it can be compared with the corresponding plot of the no-absorber case. The data for the five-centimeter-lead case are given in Table IV for the positive and negative particles, and for the combination in Table III. The normalization factor for this case is  $0.142 \text{ ster}^{-1} \text{ cm}^{-2}$ .

The case involving twenty centimeters of lead above the chamber contained only a third as much data as the other two cases, and, furthermore, the exposures were made on Eastman Linograph Panchromatic film, which proved to be too grainy for



MOMENTUM SPECTRA  
AT 3.4 KILOMETERS  
5 CM ABSORBER  
NO ABSORBER



good momentum measurements. The plot of these data is not too meaningful statistically, but, so far as can be told, the distribution does not differ appreciably from that obtained in the five-centimeter case.

### C Heavily Ionizing Particles

In measuring the curvature of the tracks, a number of tracks corresponding to particles with an ionization density well above minimum were noticed. In an effort to determine the spectrum and identity of the particles producing these tracks, all data were utilized, including the seven rolls taken with a field of 10,000 gauss and those rolls considered to be too light for easy measurement of tracks of minimum ionization. The total number of singly occurring tracks in this field of data was also determined so that the relative number of particles with an ionization well above minimum could be established. For the statistical analysis of the number of heavily ionizing particles present in a particular case, no length criterion was established while for the momentum spectrum of the particles a minimum length of twelve centimeters in the chamber was used.

Of 5040 single tracks examined for the no-absorber case, ninety-nine, or 2.0 percent, were heavily ionizing. Similarly, for 2940 single tracks under five centimeters of lead fifty, or 1.5 percent, were found to be heavily ionizing, while under twenty centimeters of lead the corresponding

figures are 1560 and twelve, which is 0.8 percent. Of the 161 heavily ionizing tracks for the three cases, all but three show a direction of curvature corresponding to a positive particle moving downward.

The data for the heavily ionizing particles twelve centimeters long or longer of both the no-absorber case and the five-centimeter-lead-absorber case are given in Table V. Since two field strengths were used, the curvature had to be converted to momentum before summing the particles, and thus the data are given in terms of the number of particles found in a particular momentum interval. Plate XXI is a plot of these data. The distribution had been drawn to zero for the lowest momentum found for any heavily ionizing particle. Within statistics the momentum distributions for those heavily ionizing particles found under no absorber and five centimeters of lead do not differ, and thus the two are plotted together to improve the statistics and to show the low momentum cutoff, which, as will be shown later, does not depend upon the nature of the absorber above the chamber. In order to show the ionization density of the protons in the range of momentum considered in Plate XXI, the ratio  $I/I_m$  has been plotted as a second abscissa. This is the ratio of the ionization density of a proton as compared with minimum ionization

MOMENTUM SPECTRUM  
OF HEAVILY IONIZING  
PARTICLES (PROTONS)

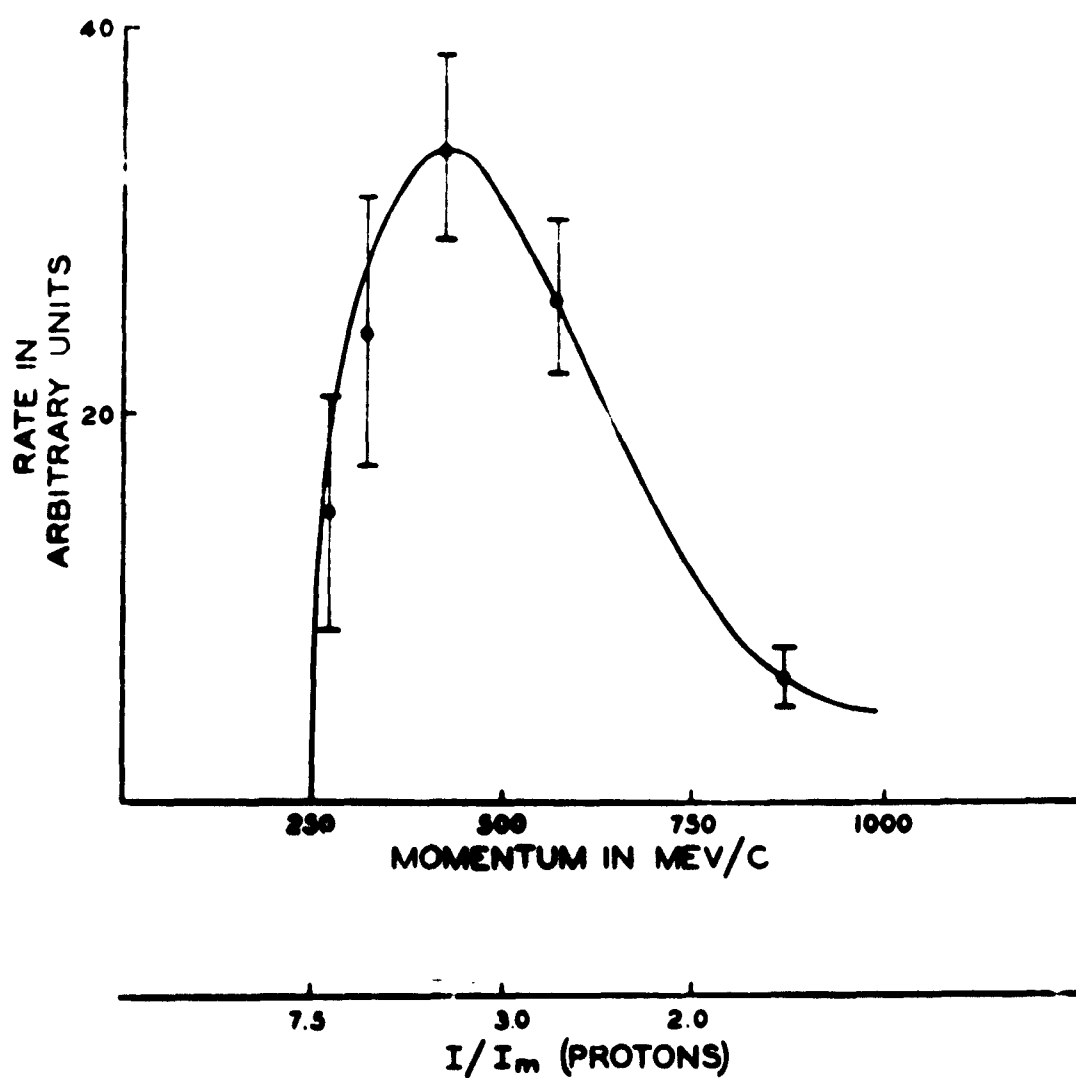


TABLE 11

TABULATED DATA FOR POSITIVE AND NEGATIVE PARTICLES  
OF THE NO-ABSORBER CASE AND THE 5 CM LEAD CASE

Radius of Curv. in Meters	No Absorber Case		5 cm Lead Case	
	Positive	Negative	Positive	Negative
.316	11	5	3	2
.316	8	11	1	0
	6	4	1	2
.400	13	7	2	0
	7	10	2	3
.515	7	7	1	2
	1	3	0	1
.583	7	11	1	1
	2	1	3	0
.661	9	13	4	1
	3	2	0	1
.751	16	10	2	3
	4	1	3	1
.852	12	7	2	4
	1	1	4	2
.966	6	2	5	6
	4		1	5
1.09	9		7	4
	4	1	2	5
1.23	9	12	5	5
	7	2	7	4
1.39	13	11	13	2
	7	6	2	3
1.56	8	6	10	9
	7	4	9	5
1.74	16	15	18	5
	7	3	5	2
1.94	16	13	16	10
	8	9	3	2
2.16	12	20	14	6
	15	2	2	3
2.42	19	11	13	9
	9	11	13	6
2.73	20	6	19	11
	16	8	5	5
3.08	15	11	24	12
	13	11	11	3
3.51	22	12	27	17
	17	10	21	9
4.06	21	7	33	16
	15	9	22	10



TABLE II (continued)

<u>Radius of Curv in Meters</u>	<u>No Absorber Case</u>		<u>5 cm Lead Case</u>	
	Positive	Negative	Positive	Negative
4.81	27	22	28	26
	39	17	24	19
5.85	12	14	41	20
	20	18	32	23
7.81	22	12	48	26
	24	15	28	11
10.00	98	49	79	70
10.00	98	85	90	88

TABLE III

THE DISTRIBUTION IN MOMENTUM FOR PARTICLES OF BOTH  
SIGNS FOR THE NO ABSORBER CASE AND THE 5 CM LEAD CASE

<u>Momentum in Mev/c</u>	<u>5 cm Lead Case</u>		<u>No Absorber Case</u>	
40	2.7	--	12.6	2.5
160	11.4	1.5	45.7	3.3
315	19.1	2.1	30.2	2.9
465	24.5	2.5	32.3	3.0
655	17.6	1.7	26.0	2.2
890	18.9	1.7	18.3	1.8
1240	14.8	1.0	13.8	1.1
1980	9.3	0.6	8.2	0.5

TABLE IV

THE DISTRIBUTION IN MOMENTUM FOR  
POSITIVE AND NEGATIVE PARTICLES FOR THE 5 CM LEAD CASE

<u>Momentum in Mev/c</u>	<u>Positive Particles</u>		<u>Negative Particles</u>	
40	1.6	---	0.9	---
160	6.1	1.2	5.2	1.0
315	10.6	1.5	8.5	1.4
465	14.9	1.8	9.6	1.5
655	11.0	1.3	6.6	1.0
890	12.7	1.3	6.2	0.9
1240	8.9	0.8	5.9	0.6
1980	5.8	0.4	3.6	0.4

TABLE V  
HEAVILY IONIZING TRACKS UNDER  
NO ABSORBER AND 5 CM OF LEAD ABSORBER

<u>Momentum Range in Bev/c</u>	<u>Number of Particles</u>
0.00-0.25	0
0.24-0.30	7
0.30-0.35	12
0.35-0.50	49
0.50-0.65	39
0.65-0.88	27
1.00	10

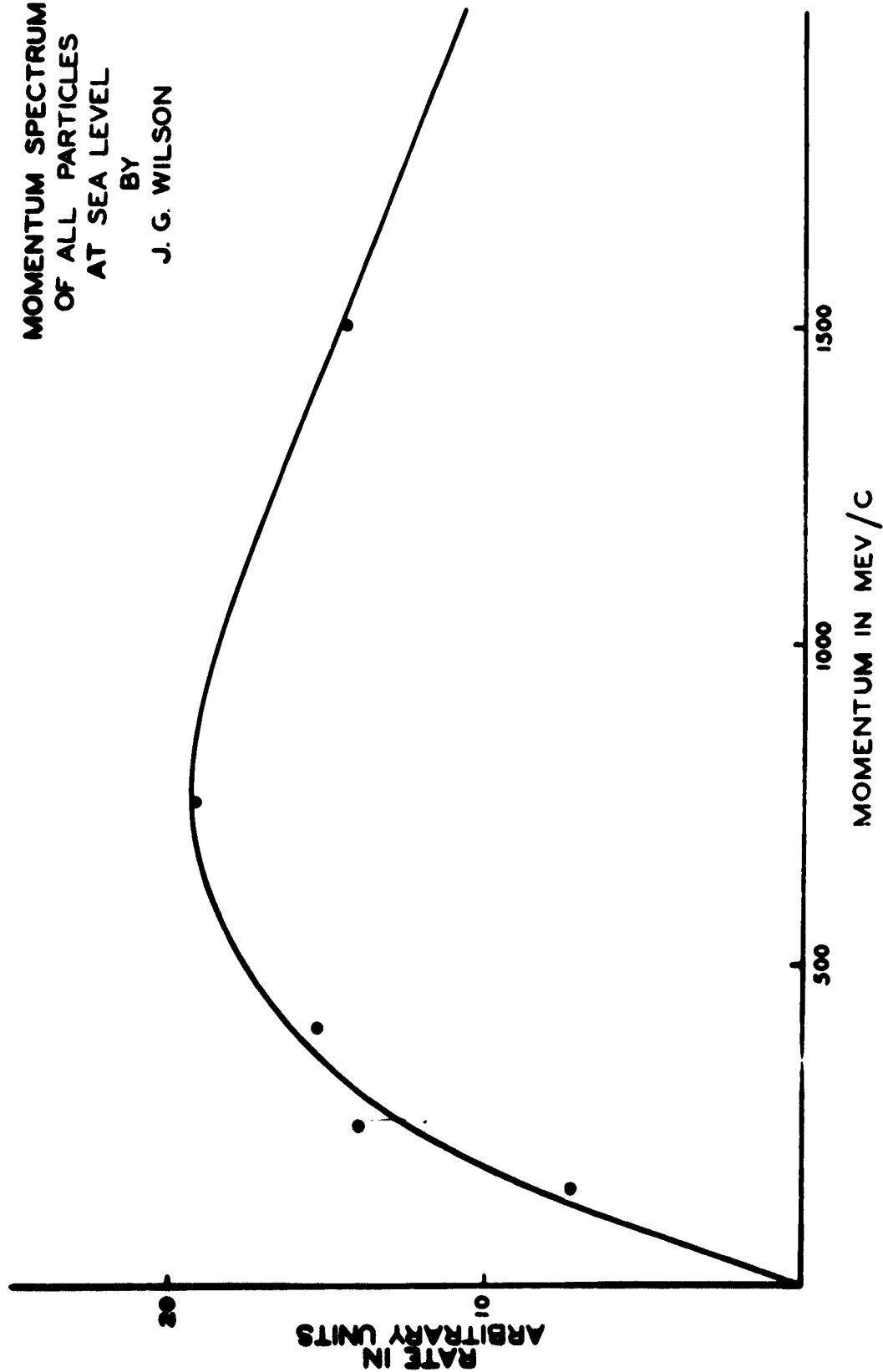
## IX DISCUSSION

## A. Momentum Distribution

The momentum distributions obtained in this case are interesting in that they are intermediate in altitude and, when compared with other similar measurements, permit a reasonably clear interpretation of the variations in the mesonic and protonic components of cosmic rays. Momentum distributions from magnetic cloud chamber measurements at sea level and at 30,000 feet have been given by Wilson (Reference 6 Plate XXII) and by Adams, Anderson, et al (Reference 2 Plate XXIII). In the case of Wilson's sea-level measurements, sufficient absorber was placed above the chamber to insure cascade multiplication of electrons, which could then be eliminated by discarding events in which more than one particle appeared. The distribution obtained by him may be considered to consist essentially of the mesonic component, since it is known that only few protons are present at sea level. The result obtained for the five-centimeter lead case in this investigation is very similar to that found by Wilson. It can be seen that the peak of the rather broad maximum of the distribution occurs at about the same point (500 Mev/c for this work and 750 Mev/c for Wilson's) and that the rate of decrease at higher momenta is comparable. It would thus appear that the momentum spectrum has not been altered much in the increase in elevation between these two observations, even though the present work does contain a fairly large number of protons.

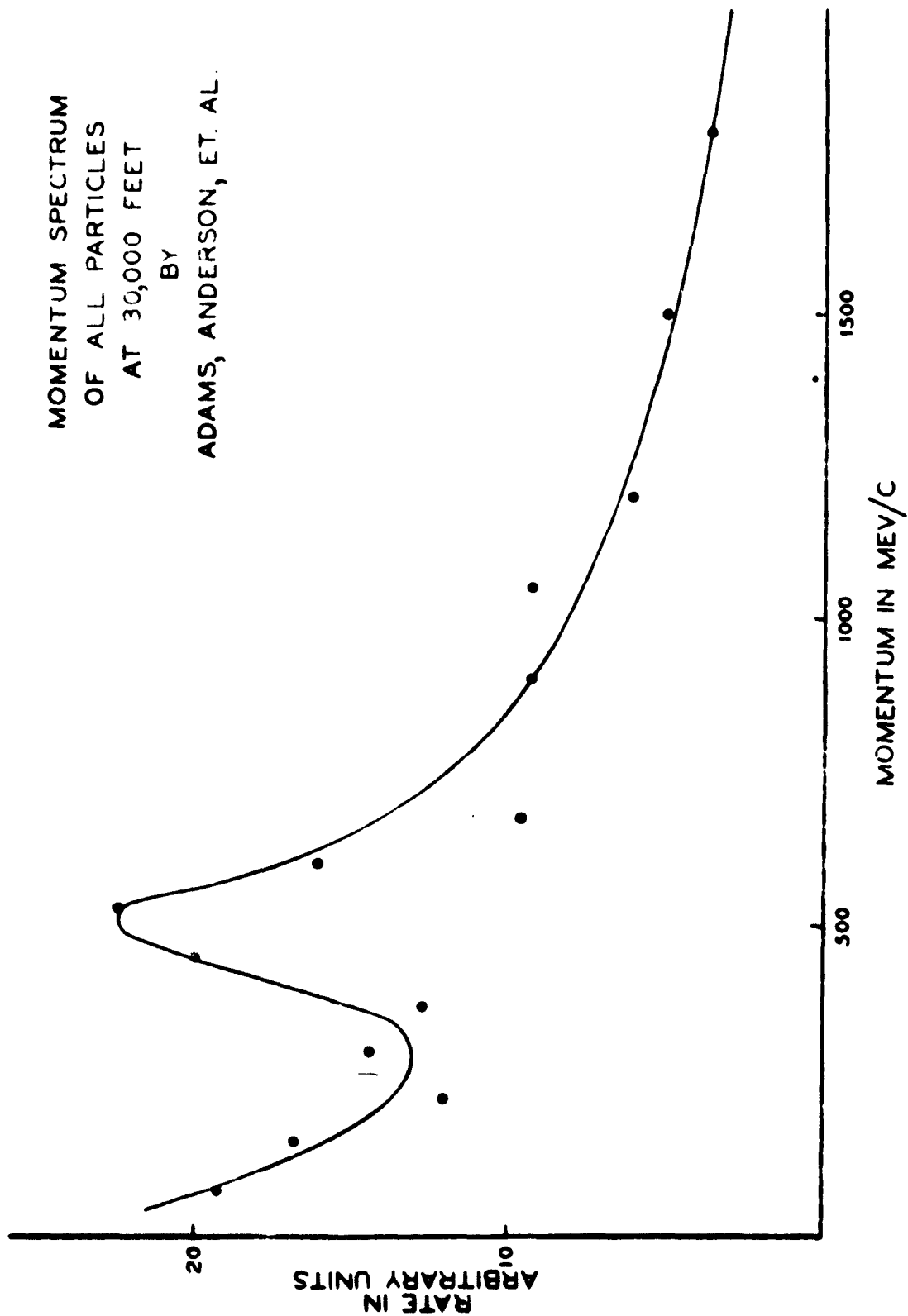
MOMENTUM SPECTRUM  
OF ALL PARTICLES  
AT SEA LEVEL

BY  
J. G. WILSON



MOMENTUM SPECTRUM  
OF ALL PARTICLES  
AT 30,000 FEET

BY  
ADAMS, ANDERSON, ET. AL.



Since the data of this investigation do not extend to high momenta as in the work of Wilson (6), Jones (7), or Blackett (8), it is impossible to deduce the form of the decrease of intensity with momentum beyond the maximum as is done by these investigators for the sea-level spectrum. It is possible, however, to get some idea of what such a spectrum might be from a knowledge of the total number of particles extending from 2.5 Bev/c to infinity. The results of this investigation show that the fraction of particles represented by the integrated intensity beyond 2.5 Bev/c is 36 percent, whereas Wilson finds 40 percent. There is no difference within statistics, and it is therefore not too improbable that the form of the spectrum is very nearly the same, even at much higher values of momenta.

The momentum spectrum obtained by Adams, Anderson, et al at 30,000 feet is much different from that obtained here. The very large number of particles found by these investigators in the low momentum end of the spectrum is undoubtedly due to the presence of large numbers of electrons, since no absorber other than the chamber wall and the upper geiger tube was present. The experimental conditions are almost exactly those prevailing in the no-absorber experiment of this investigation, and their momentum distribution should be compared with Plate XIX of this work, in which large numbers of electrons at low momenta are also found.

The main difference between the two spectra then occurs at about 500 Mev/c (magnetic rigidity of about  $1.7 \times 10^6$  gauss centimeters). At this point, although both investigations show a peak, the one obtained at 30,000 feet is much sharper and is confined to the positive particles. In the 3.4-kilometer data, however, the peak occurs in both the positive and the negative spectra. At 3.4 kilometers this peak is interpreted as being due to mesons, but such an interpretation cannot be valid for the 30,000-foot data. Since the peak occurs only in the positives, and since the cutoff at the low end is quite abrupt and is at a value of momentum just necessary for a proton to pass through the cloud chamber and trip the lower geiger counter, the natural interpretation is that the peak represents large numbers of fairly low momentum protons which, without the instrumental cutoff, might well have extended to even lower momenta. The cloud chamber used in the investigation at 30,000 feet had a rather large brass casting at the bottom and thus presented a large amount of absorber. The protons with just sufficient momentum in the chamber to penetrate to the lower geiger counter do not have an ionization density sufficiently above minimum to identify them by this means.

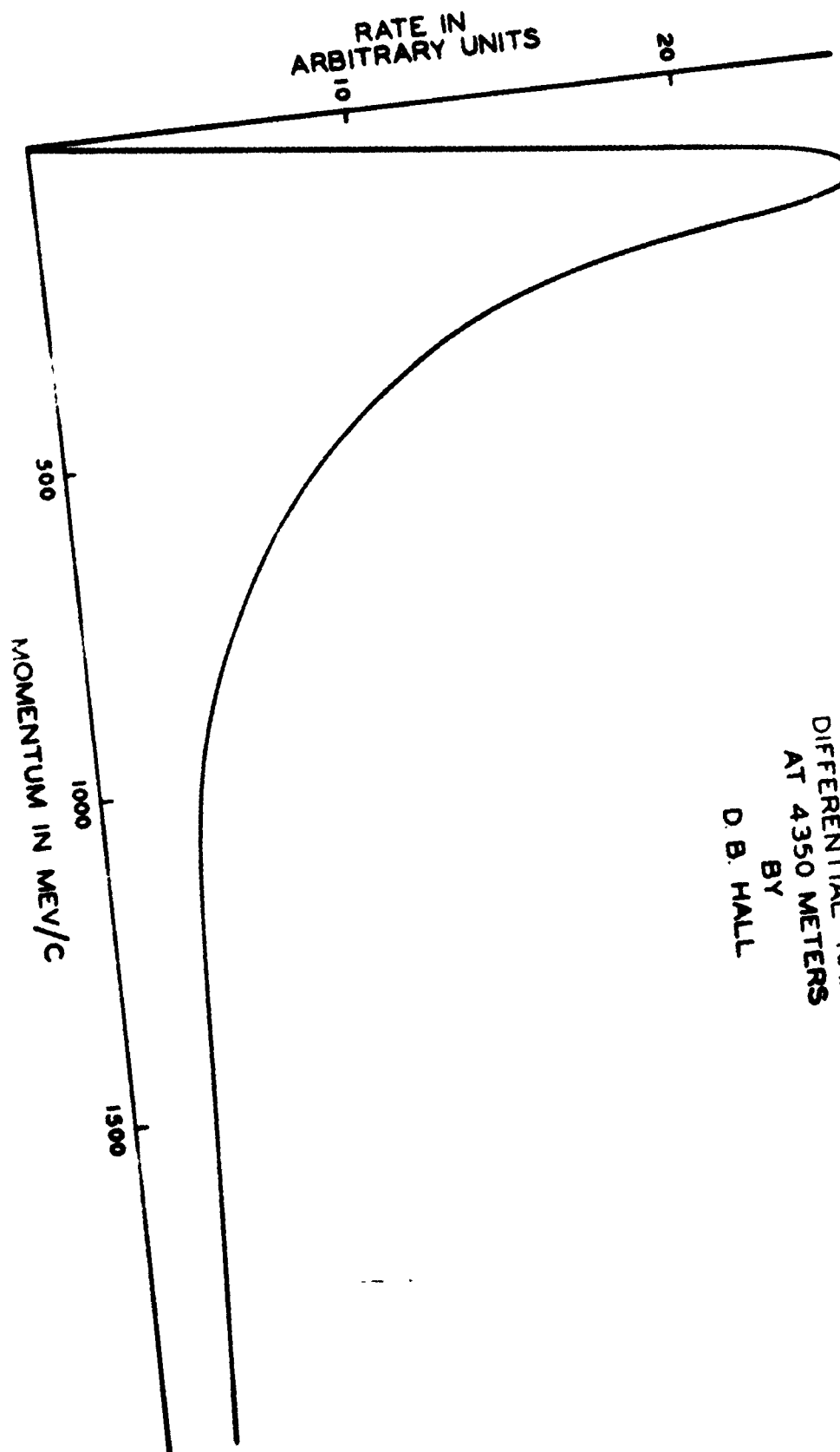
The positive excess computed from the 30,000-foot data, though not statistically meaningful, appears to be considerably in excess of that found at the lower altitudes. If the interpretation of the peak found at 500 Mev/c as being due to protons is correct, then a large part of the increase in positive

excess noted at 30,000 feet can be attributed to the protons. It is conceivable that it is all due to the protonic component.

The only momentum spectrum consisting of a sufficiently large body of data, and hence having sufficient detail to be compared with the present work, and done at a nearly equivalent altitude is that obtained by Hall (3), Plate XXIV. It is difficult however, to compare Hall's counter-telescope result directly with the magnetic cloud chamber results. Hall's work was conducted at 14,000 feet and consisted of determining the integral range spectrum by use of lead absorbers and geiger counters. This integral range spectrum can then be transformed to a differential momentum spectrum by assuming that all particles represented have the same mass. Hall assumed that all of the particles contributing to the measurement were mesons, the electrons having been eliminated in a direct manner at the larger ranges, and a correction factor computed for the lower ranges. As can be seen from Plate XXIV, the spectrum obtained by Hall has a large number of low momenta particles and shows a rather sharp maximum at 200 Mev/c. Since the position of this peak is of importance, a rather detailed discussion of possible errors is given below.

In the measurement of an integral range spectrum for the non-electronic component, the greatest difficulties are encountered for small range, where electrons cannot be eliminated easily. Hall employed a special experimental arrangement in order to obtain the small range portion of the curve





MOMENTUM SPECTRA  
TRANSFORMED FROM  
DIFFERENTIAL RANGE  
AT 4350 METERS

BY  
D. B. HALL

more accurately, but even so, large corrections had to be made to eliminate the effects of showers and electrons. It is thus quite possible that considerable numbers of electrons were included in the small range portion of the integral range spectrum, and it is in just this region that the differences between the spectra become pronounced.

Further, Hall had to assume that all of the particles contained in his integral range spectrum were mesons. This was known not to be valid, but the number of protons was thought to be so small as not to affect materially the transformation. If there are comparatively large numbers of protons present, and they are transformed from range to momentum on the basis of the range-momentum relationship for mesons, the intensity which they contribute is displaced to lower momenta, and thus they give a larger contribution to a smaller momentum band than they actually occupy. On the basis of the proton intensity and its probable composition computed in this work, there does not appear to be a sufficient number of protons to account completely for the differences observed in the spectra. It may well be, however, that considerably more protons are present at the higher elevation. This seems plausible when considering the vast increase found by Adams, Anderson, et al at 30,000 feet.

The momentum spectrum obtained by Hall is extremely unstable where its variation with altitude is considered. This suggests that a large amount of local production is

contributing to the meson peak observed. If this were so, it does not seem reasonable that the production should drop abruptly to unnoticeable proportions in the interval from 14,000 feet to 11,000 feet. This hypothesis is made almost untenable by the later work of Carr, Schein, and Barbour (13) in which, from observations at 18,000 feet, they estimate the production necessary to yield a spectrum comparable with Hall's. They find that the production must be equivalent to fourteen percent of the mesonic radiation able to penetrate ten centimeters of lead at their observation point. Such a high production rate is not found by them at 18,000 feet, and since the spectrum at 11,000 feet does not show the large quantities of low energy mesons observed by Hall, it must be concluded that if the answer to the anomaly resides in local low momenta meson production, it is limited to an extremely narrow layer of the atmosphere.

Of all of the possible reasons for finding a large number of low momentum particles in the computed transformation, the most appealing is that a sufficient number of protons with a range-momentum relationship vastly different from that of mesons, especially at just the low momenta considered, are present, and hence the entire difficulty lies in not knowing just how many protons are contributing. The discrepancy can be almost accounted for by a protonic component having an intensity of about 25 percent of the mesonic radiation. Further evidence gathered by this group in a later

experiment supports the idea that protons are present in this abundance.

A comparison of the spectrum obtained at 3.4 kilometers under no absorber and under five centimeters of lead is of interest because of the possibility for investigating the number of electrons which are included in such an investigation when electron removal is not assured by a cascade process. As can be seen from Plate XIX, which includes both spectra, electrons are included up to about one Bev/c. There is no particular reason why electrons of higher momenta should not also be observed in the plot if they were present in the radiation, and hence it can be assumed that the electronic component has a quite small intensity when compared with the mesonic component for momenta above about one Bev/c.

#### B. Positive Excess

Much interest has centered on the question of the excess of positive particles over negative in cosmic radiation. It is of primary importance, since such an excess in the mesonic component offers another experimental check point on meson production theory. Many observers have measured the positive excess at sea level. Jones (7) and Hughes (9) using a cloud chamber method found  $1.18 \pm 0.08$  and  $1.29 \pm 0.05$  respectively. Using a magnetic lens Brode (10) found a value of  $1.32 \pm 0.02$ . Conversi (11,12) has obtained values near these using both a magnetic lens and a delayed coincidence

scheme. The rather wide spread of data considering the errors quoted, is probably a reflection of the geomagnetic latitude as well as the different methods of measurements.

At higher altitudes, very little data is available, and, in general, the high-altitude data, due to the difficulties of measurement, suffer from rather large statistical uncertainties. Anderson has found a large increase in the positive excess with increasing altitude, the most significant indication coming from the work at 30,000 feet. The present work confirms the increase in positive excess with increasing altitude.

Plate XX shows the momentum spectrum for both positive and negative particles as found at 3.4 kilometers under five centimeters of lead. As can be seen, there is no definite trend of variation of positive excess with momentum. The positive excess of  $1.5 \pm 0.1$  is computed for those particles having a momentum lying between fifty Mev/c and 2.5 Bev/c. As explained previously, almost all electrons have been removed from this spectrum.

It is difficult to understand why the ratio of positive to negative mesons should vary with altitude. It is thought that the mu mesons have no appreciable nuclear interactions, and hence the spectrum at one altitude should be computable from that of another altitude with no asymmetry between positive and negative particles. In particular, the transformation from 3.4 kilometers to sea level involves a momentum loss of

about 600 Mev/c for particles of high momenta and a decay loss which varies with momentum, becoming inappreciable at momenta of the order 1.5 Bev/c and higher. The entire upper portion of the momentum spectrum of Plate XX should then be able to be transformed to sea level by simply shifting the abscissa by about 600 Mev/c. However, it is known that the positive excess in a region from one to two Bev/c at sea level is about 1.3, and one must thus conclude that:

- (a) there is production of large numbers of negative mesons in the interval
- (b) the positives are preferentially removed, or
- (c) particles other than mesons are involved.

The first hypothesis is untenable because of the lack of appreciable production found at higher altitudes, and, of course, it would be hard to understand why there should suddenly be an excess of negatives over positives in the production, when at higher altitudes the reverse was true.

Although there is an asymmetry in the decay time of the meson between positive and negative mesons, this occurs when the meson is essentially at rest, and, of course, is the other way around, with the negative meson showing the smaller effective half life.

The last hypothesis appears to be the most probable. It is known that there are some protons present at the higher elevation, and only a few at sea level. The removal of protons from the spectrum can be understood on the basis of their nuclear interaction. For the shower-producing radiation (at

least a part of which is protonic) Cocconi (14) finds a mean interaction path length of about  $120 \text{ gm/cm}^2$ . The layer of air absorber traversed by a particle from the elevation at Climax to sea level is equal to about three such interaction lengths. If each interaction removes the proton, or leaves it with insufficient range to traverse the absorber (as would be the case with protons of momenta approximately two Bev/c), then the proton intensity should be reduced by about a factor of ten. On the other hand, the hard component is found to decrease by only a factor of two.

If for the moment it be considered that the mesonic component at sea level has a positive excess of 1.3, and this is constant with increasing altitude, then at 3.4 kilometers there would have to be an intensity of protons equal to 8 percent of the total hard component intensity in order to account for a positive excess of 1.5. Since in this investigation it was found that the recognizable protons constituted about 2 percent of the total radiation, it is not at all impossible that another 6 percent are present, but cannot be identified because of a higher momentum, and hence an ionization density nearer minimum. In fact, it is not at all unreasonable to suspect that a small portion of the sea-level positive excess can be attributed to protons.

### C. Protons

Plate XXI gives the distribution in momentum of heavily ionizing particles, combining those observed under no absorber and under five centimeters of lead. Only those tracks distinctly more dense than the average run of tracks were included in this plot. Although the selection was of necessity quite arbitrary, it was found that for particles having a momentum less than 500 Mev/c, several different observers agreed almost absolutely on those tracks to be included. As can be seen from Plate XXI, this value of momentum corresponds with an ionization density of about three times minimum. Although the group of heavily ionizing tracks was selected on the basis of track density alone, it was found that all but three had a direction of curvature corresponding to a positive particle moving downward, thus giving added credence to the interpretation of these tracks as protons.

The remarkably sharp cutoff at low momenta is an instrumental effect. Since the events were selected by means of counters placed above and below the chamber, a particle had to go through the lower wall of the chamber and enter the lower geiger counter in order to be observed. The mass of absorber represented by the apparatus was computed and found to be equal to  $1.2 \text{ gm/cm}^2$  of aluminum. From this the proton cutoff was found to be about 250 Mev/c. No heavily ionizing particles were found with momenta less than 250 Mev/c, again verifying the assumption that the particles being considered are protons.



It can also be concluded that, if particles of an intermediate mass of the order of 500 to 1000 electron masses are present, they must represent an extremely small fraction of the intensity of radiation at this altitude.

In order to compute the contribution of protons to the total intensity, it can be assumed that the region 350 to 500 Mev/c is unaffected by either low momentum cutoff or by failure to recognize the protons because of a low ionization density. The intensity of protons thus found in the interval 350 to 500 Mev/c for the no-absorber case is 10 percent of the intensity of the non-electronic component found in this same momentum interval under five centimeters of lead. If no production and no losses other than ionization losses are assumed for the protons penetrating five centimeters of lead, a computation involving the range-momentum relationship for protons in lead shows that some 20 percent of the radiation in a momentum band centered at 600 Mev/c consists of protons. The assumption of no losses other than ionization losses is, of course, not valid, but it is probable that there is also some production, and the exact contribution of protons at the higher momenta is thus subject to large error when computed in this way.

From even the meager data available on protons obtained in this investigation, the assumption that the relative increase of positive particles over negative particles with increase in altitude is seen to be justified. If the contribution of the protonic component to the radiation does not

fall too rapidly at the higher momenta, it can be seen that even a portion of the "normal" positive excess found at sea level may be due to protons.

## X. SUMMARY

(1) The momentum spectrum of the non-electronic ionizing component of cosmic radiation for momenta between 100 Mev/c and 2.5 Bev/c for both the positive and negative particles, filtered through five centimeters of lead, has been obtained. It is found to be quite similar to the sea-level spectrum in this momentum interval. Although little information can be obtained from this work concerning higher momenta, the ratio of particles of momentum higher than 2.5 Bev/c to those below 2.5 Bev/c is the same within statistics as that at sea level.

(2) The momentum spectrum for momenta between 100 Mev/c and 2.5 Bev/c for the ionizing component of the cosmic radiation has been found with the electronic component not removed. In comparison with the spectrum in which the electronic component has been removed, it is found that the electron contribution extends to about one Bev/c.

(3) Fairly large numbers of protons have been found. There are enough protons at the lower momenta to account for the increase in the positive excess from sea level to 3.4 kilometers. At slightly higher momenta it has been computed that there are enough protons to completely account for the positive excess.

(4) No evidence was found for a particle of mass 1000 electron masses, indicating that, if present at 3.4 kilometers, they are rare as compared with protons.

## DISTRIBUTION LIST

### Professional

Dr. W. F. A. Swann, Director  
Bartol Research Foundation  
Franklin Institute  
Swarthmore, Pennsylvania

Prof. C. C. Lauritsen  
Department of Physics  
California Institute of Technology  
Pasadena, California

Prof. J. D. Anderson  
Department of Physics  
California Institute of Technology  
Pasadena, California

Prof. R. I. Brode  
Department of Physics  
University of California  
Berkeley 4, California

Prof. E. O. Lawrence  
Radiation Laboratory  
University of California  
Berkeley 4, California

Prof. J. R. Richardson  
Department of Physics  
University of California  
(Los Angeles)  
Los Angeles 2, California

Prof. E. C. Grentz  
Department of Physics  
Carnegie Institute of Technology  
Schenley Park  
Pittsburgh 13, Pennsylvania

Dr. M. A. Tuve  
Department of Terrestrial Magnetism  
Carnegie Institution of Washington  
Washington, D. C.

Dr. R. S. Shankland  
Case Institute of Technology  
Department of Physics  
University Circle  
Cleveland 6, Ohio

Prof. S. K. Allison  
Institute of Nuclear Studies  
University of Chicago  
Chicago, Illinois

Prof. J. Rainwater  
Columbia University  
Radio-Isotopes Laboratories  
P. O. Box 111  
Irvington-on-Hudson, New York

Prof. R. E. Wilson  
Laboratory of Nuclear Studies  
Cornell University  
Ithaca, New York

Prof. W. M. Nielson  
Department of Physics  
Duke University  
Durham, North Carolina

Dr. Jay Sells  
Research Laboratory  
General Electric Company  
Schenectady, New York

Dr. Milton Jay  
Department of Physics  
George Washington University  
Washington, D. C.

Prof. W. F. Ramsey  
Department of Physics  
Harvard University  
Cambridge, Massachusetts

Director  
Nuclear Laboratory  
Harvard University  
Cambridge, Massachusetts

Prof. F. W. Loomis  
Department of Physics  
University of Illinois  
Urbana, Illinois

Prof. A. C. G. Mitchell  
Department of Physics  
Indiana University  
Bloomington, Indiana

Prof. J. A. Van Allen  
Department of Physics  
State University of Iowa  
Iowa City, Iowa

Prof. J. D. Stranathan  
Department of Physics  
University of Kansas  
Lawrence, Kansas

Prof. J. M. Cork  
Department of Physics  
University of Michigan  
Ann Arbor, Michigan

Prof. W. E. Hazen  
Department of Physics  
University of Michigan  
Ann Arbor, Michigan

Prof. E. H. Williams  
Department of Physics  
University of Minnesota  
Minneapolis, Minnesota

Prof. E. P. Ney  
Department of Physics  
University of Minnesota  
Minneapolis, Minnesota

Prof. Truman S. Gray  
Servo-Mechanisms Laboratory  
Massachusetts Institute of Technology  
Cambridge 39, Massachusetts

Professor J. R. Zacharias. . . . (2)  
Laboratory for Nuclear Science and  
Engineering  
Massachusetts Institute of Technology  
Cambridge 39, Massachusetts

Prof. S. A. Korff  
Department of Physics  
New York University  
University Heights  
New York 53, New York

Prof. E. Waldman  
Nuclear Physics Laboratory  
University of Notre Dame  
Notre Dame, Indiana

Prof. J. N. Cooper  
Department of Physics  
Ohio State University  
Columbus 10, Ohio

Prof. W. E. Stephens  
Department of Physics  
University of Pennsylvania  
Philadelphia 4, Pennsylvania

2 Prof. A. J. Allen  
Department of Physics  
University of Pittsburgh  
Pittsburgh, Pennsylvania

Prof. G. T. Reynolds  
Department of Physics  
Princeton University  
Princeton, New Jersey

Prof. M. I. White  
Department of Physics  
Princeton University  
Princeton, New Jersey

Prof. Leticia del Rosario  
Department of Physics  
Gobierno De Puerto Rico  
Universidad De Puerto Rico  
Rio Piedras  
Puerto Rico

Prof. K. Lark-Horovitz  
Department of Physics  
Purdue University  
Lafayette, Indiana

Dr. T. W. Bonner  
Department of Physics  
Rice Institute  
Houston, Texas

Prof. A. E. Marshak  
Department of Physics  
University of Rochester  
Rochester, New York

Prof. Charles A. Whitmer  
Chairman, Department of Physics  
Rutgers University  
New Brunswick, New Jersey

Prof. E. L. Hinzton  
Microwave Laboratory  
Stanford University  
Palo Alto, California

Prof. F. Bloch  
Department of Physics  
Stanford University  
Palo Alto, California

Prof. J. D. Trimmer  
Department of Physics  
University of Tennessee  
Knoxville, Tennessee

4

Prof. A. L. Hughes  
Department of Physics  
Washington University  
St. Louis, Missouri

Prof. R. J. Sard  
Department of Physics  
Washington University  
St. Louis, Missouri

Prof. J. R. Manley  
Department of Physics  
University of Washington  
Seattle 5, Washington

3

Mr. J. W. Coltman  
Research Laboratories  
Westinghouse Electric Corporation  
East Pittsburgh, Pennsylvania

Prof. R. A. Herb  
Department of Physics  
University of Wisconsin  
Madison 6, Wisconsin

Prof. W. M. Watson . . . . . (2)  
Department of Physics  
Sloane Physics Laboratory  
Yale University  
New Haven, Connecticut

#### Governmental

Chief of Naval Research . . . . (2)  
Attn: Nuclear Physics Branch  
Navy Department  
Washington 25, D. C.

Director, Naval Research Laboratory (9)  
Attn: Technical Information Officer  
Washington 25, D. C.

Director  
Office of Naval Research  
Chicago Branch Office  
844 North Rush Street  
Chicago 11, Illinois

Director  
Office of Naval Research  
San Francisco Branch Office  
801 Donahue Street  
San Francisco 24, California

Director  
Office of Naval Research  
New York Branch Office  
346 Broadway  
New York 13, New York

Director  
Office of Naval Research  
Pasadena Branch Office  
1030 East Green Street  
Pasadena 1, California

Officer in Charge . . . . . (10)  
Office of Naval Research  
Navy No. 100  
Fleet Post Office  
New York, New York

Superintendent, Nucleonics Division  
Naval Research Laboratory  
Anacostia, Washington, D. C.

Chief, Bureau of Ships  
Attn: Code 390  
Navy Department  
Washington 25, D. C.

Chief, Bureau of Ships  
Attn: Code 330  
Navy Department  
Washington 25, D. C.

Chief, Bureau of Ordnance  
Attn: Rem  
Navy Department  
Washington 25, D. C.

Chief, Bureau of Ordnance  
Attn: Re9a  
Navy Department  
Washington 25, D. C.

Chief, Bureau of Aeronautics  
Attn: RS-5  
Navy Department  
Washington 25, D. C.

Chief, Bureau of Aeronautics  
Attn: Technical Library  
Navy Department  
Washington 25, D. C.

Commanding Officer  
Naval Radiological Defense Laboratory  
San Francisco Naval Shipyard  
San Francisco 24, California

Chief of Naval Operations  
Attn: Op 36  
Navy Department  
Washington 25, D. C.

Commander, U. S. Naval Ordnance Test  
Station  
Technical Library  
Inyokern, China Lake, California

Commanding General  
Air Force Cambridge Research Center  
Attn: Geophysics Research Library  
230 Albany Street  
Cambridge 39, Massachusetts

Senior Scientific Advisor  
Office of the Under Secretary  
of the Army  
Department of the Army  
Washington 25, D. C.

Director, Research and Development  
Division  
General Staff  
Department of the Army  
Washington 25, D. C.

Chief, Physics Branch  
U. S. Atomic Energy Commission  
1901 Constitution Avenue, N. W.  
Washington 25, D. C.

U. S. Atomic Energy Commission  
Attn: Roland Anderson  
Patent Branch  
1901 Constitution Avenue, N. W.  
Washington 25, D. C.

U. S. Atomic Energy Commission . . (4)  
Library Branch  
Technical Information Division, ORE  
P. O. Box E  
Oak Ridge, Tennessee

Oak Ridge National Laboratory  
Attn: Head, Physics Division  
P. O. Box P  
Oak Ridge, Tennessee

Brookhaven National Laboratory  
Attn: Dr. S. C. Stanford  
Research Library  
Upton, L. I., New York

Oak Ridge National Laboratory  
Attn: Central Files  
P. O. Box P  
Oak Ridge, Tennessee

Argonne National Laboratory  
Attn: Hoylande D. Young  
P. O. Box 5207  
Chicago 90, Illinois

Document Custodian  
Los Alamos Scientific Laboratory  
P. O. Box 1663  
Los Alamos, New Mexico

Technical Information Group  
General Electric Company  
P. O. Box 100  
Richland, Washington

Carbide and Carbon Chemical Division  
(K-25 Plant)  
Plant Records Department  
Central Files (K-25)  
P. O. Box P  
Oak Ridge, Tennessee

Carbide and Carbon Chemical Division  
(Y-12 Plant)  
Central Reports & Information (Y-12)  
P. O. Box P  
Oak Ridge Tennessee

Ames Laboratory  
Iowa State College  
P. O. Box 14A, Station A  
Ames, Iowa

Knolls Atomic Power Laboratory  
Attn: Document Librarian  
P. O. Box 1072  
Schenectady, New York

Mound Laboratory  
Attn: Dr. M. M. Haring  
U. S. Atomic Energy Commission  
P. O. Box 32  
Miamisburg, Ohio

Sandia Corporation  
Sandia Base  
Attn: Mr. Dale N. Evans  
Classified Document Division  
Albuquerque, New Mexico

U. S. Atomic Energy Commission  
Attn: Division of Technical Information  
and Declassification Service  
New York Operations Office  
P. O. Box 30  
Ansonia Station  
New York 23, New York

National Bureau of Standards Library  
Room 204, Northwest Building  
Washington 25, D. C.

National Science Foundation  
2114 California Street  
Washington 25, D. C.

Commanding General  
Air Research & Development Command  
Attn: R RRP  
P. O. Box 1359  
Baltimore 13, Maryland

Director, Office of Ordnance Research  
2127 Myrtle Drive  
Durham, North Carolina

Director  
Office of Naval Research  
Boston Branch Office  
150 Causeway Street  
Boston, Massachusetts

Foreign

Doctor Cesar Lattes  
Scientific Director, Brazilian Center  
of Physical Research  
Rio de Janeiro, Brazil